Review

Fourier Transform Infrared (FTIR) Spectroscopy for Measurements of Vehicle Exhaust Emissions: A Review

Barouch Giechaskiel * and Michaël Clairotte

European Commission—Joint Research Centre (JRC), 21027 Ispra, Italy; michael.clairotte@ec.europa.eu
* Correspondence: barouch.giechaskiel@ec.europa.eu; Tel.: +39-0332-785-312

Featured Application: The review showed that sampling with FTIR from the tailpipe of vehicles for the determination of various gaseous pollutants is a possible alternative to currently regulated techniques.

Abstract: Pollution from vehicles is a serious concern for the environment and human health. Vehicle emission regulations worldwide have limits for pollutants such as hydrocarbons, CO, and NO_x. The measurements are typically conducted at engine dynamometers (heavy-duty engines) sampling from the tailpipe or at chassis dynamometers (light-duty vehicles) sampling from the dilution tunnel. The latest regulations focused on the actual emissions of the vehicles on the road. Greenhouse gases (GHG) (such as CO_2, CH_4, N_2O), and NH_3 have also been the subject of some regulations. One instrument that can measure many gaseous compounds simultaneously is the Fourier transform infrared (FTIR) spectrometer. In this review the studies that assessed FTIRs since the 1980s are summarized. Studies with calibration gases or vehicle exhaust gas in comparison with well-established techniques were included. The main conclusion is that FTIRs, even when used at the tailpipe and not at the dilution tunnel, provide comparable results with other well-established techniques for CO_2, CO, NO_x, while for hydrocarbons, higher deviations were noticed. The introduction of FTIRs in the regulation needs a careful description of the technical requirements, especially interference tests. Although the limited results of prototype portable FTIRs for on-road measurement are promising, their performance at the wide range of environmental conditions (temperature, pressure, vibrations) needs further studies.

Keywords: FTIR; NDIR; NDUV; CLA; NH_3; formaldehyde; acetaldehyde; PEMS

1. Introduction

Vehicle emissions are regulated since the 1970s [1]. The measurements are conducted on chassis dynamometers (light-duty vehicles) or in engine test cells (heavy-duty engines). The instruments described in the regulations are sampling from the full dilution tunnel, where the whole exhaust gas is diluted, or directly from the tailpipe (undiluted exhaust). The control of the regulated pollutants (e.g., CO, NO_x) with advanced aftertreatment devices [2] has led in some cases to increased emission of non-regulated pollutants (e.g., N_2O, NH_3). The measurement techniques for regulated pollutants are well-defined in the regulation (e.g., non-dispersive infrared (NDIR) for CO and CO_2). For non-regulated pollutants, only recently, a Global Technical Regulation for light-duty vehicles (GTR 15) prescribes possible measurement techniques. One method that can measure many compounds is FTIR (Fourier transform infrared) spectroscopy (= study of the interaction between light with matter) [3]. Many compounds absorb infrared energy at an intrinsic wave number (or wavelength) proportionally to their concentration. In an FTIR spectrometer, some of the infrared (IR) radiation is absorbed by the sample, and some of it is passed through (transmitted). The resulting molecular absorption and transmission response can be used to identify the components of the sample and their concentration. FTIR, compared to other IR techniques, can measure many components in real-time due to the use of an interferometer

that allows the collection of a broad range of wavelengths. By contrast, NDIR analyzers measure one compound due to the use of an optical filter that allows the selection of a narrow wavelength area, specific to the compound of interest.

FTIR is used in geology, chemistry, materials, medicine, and biology research fields on solid, liquid, and gaseous samples [4]. FTIR has been used in a wide range of air pollution-related studies in both ambient air and environmental chambers [5,6]. Already in the late 1970s, an FTIR system was installed in a van for air pollution measurements for the Environmental Protection Agency (EPA) of the United States of America (USA) [7,8]. FTIR has also been applied for aerosol analysis [9,10], for example, to assess the hygroscopicity of ambient particles [11] or analyze surface functional groups of particles [12]. Another application was the measurement of stack emissions from various processes, such as incinerators [13]. Other researchers have used open path FTIR to record CO, CO_2, and N_2O [14] or NH_3 [15] emissions from high traffic roadside sites or even emissions in aircraft exhaust [16]. Extractive in cell FTIR has been used in many applications, e.g., trains [17]. Extractive measurement with an activated charcoal tube was used to measure volatile organic compounds (VOC) of a heavy-duty engine [18]. Applications in atmospheric and environmental studies were reviewed elsewhere [19,20].

The application of FTIR spectroscopy to vehicles' exhaust analysis began in the early 1980s [21–23]. It received a lot of attention for the study of alternative fuels due to its ability to discriminate oxidized species in tailpipe gases [24–27]. Other studies focused on TWC (three-way catalysts) [28–30] and low ambient temperatures [27,29]. Later FTIR was used to measure emissions from NO_x reduction systems [31] due to its ability to simultaneously measure separately the oxides of nitrogen [27,32,33].

However, the technique did not spread out in the industry due to several practical problems, such as complexity of calibration (due to cross sensitivity of, e.g., CO_2 and H_2O), slow response, and poor concentration accuracy when compared to the regulated analytical techniques [31,34]. The evolution of computers and algorithms made it possible to have an instrument that can measure and analyze the data in real time. Since then, and especially in the last decade, the use of FTIR spectrometers has widespread.

It has been used for the measurement of gas concentrations for various studies, e.g., soot oxidation [35], or SCR (selective catalytic reduction for NO_x) [36,37] and catalyst evaluation [38–40] with synthetic gases. It has also been used in engine test beds to assess ethanol [41,42], biodiesel [43] such as Jatropha [44], dimethyl ether (DME) [45], or hydro-treated vegetable oil (HVO) [46], homogeneous charge compression ignition (HCCI) engines [47], gasoline compression ignition engine [48], post injection effect on emissions [49], NH_3 sensors [50], or even modeling of emissions [51]. FTIR instruments have also been used on chassis dynamometers: Small gasoline engines [52] or even diesel trucks [53,54]. For example, for exhaust gas recirculation (EGR) [55], alternative fuels [56,57], reactive nitrogen compounds [58,59], impact of low temperature on non-regulated pollutants [60], and retrofit evaluation [61,62] of diesel vehicles. Similarly, chassis dynamometer studies with gasoline vehicles [63] focused on unregulated emissions [64–68], NH_3 [69–73], effect of exhaust gas reforming on emissions [74], low temperature [60,75,76], alternative fuels [65,77], and hybrids [78–80]. Motorcycles' non-regulated pollutants emissions have also been assessed with FTIR [81–85].

The on-road application started in 2000 [86]. Since then other researchers measured emissions on the road [87–89], greenhouse gases (GHG) [90], nitrogen species [91], cold start emissions [92–96] of gasoline vehicles and the impact of ambient temperature [97]. A few also studied compressed natural gas (CNG) [98], diesel fueled vehicles [99–101] and their non-regulated pollutants [102].

Currently in the European Union (EU), FTIR is allowed for tailpipe (undiluted) NH_3 measurements for heavy duty engines (Commission Regulation (EU) 582/2011). The same applies globally with UNECE (United Nations Economic Commission for Europe) Regulation 49. It is also prescribed in the UNECE light-duty vehicles GTR 15 (Global Technical Regulation) for ethanol, formaldehyde, acetaldehyde and N_2O from the dilution

tunnel. The future Euro 7 regulation on light-duty and heavy-duty vehicles moves in a direction that these pollutants should be tested on the road [103]. Thus, using the FTIR for simultaneous analysis of various pollutants sampling from the tailpipe (undiluted exhaust) is an attractive option [104,105] that needs to be assessed.

The reviews on the topic are limited and 20 years old [31]. Furthermore, assessing FTIRs for regulatory purposes has not been discussed before. The objective of this paper is to review studies that have evaluated FTIR systems for automotive exhaust gas applications. Special emphasis is given to portable applications and low emission levels to assess the suitability for future regulations.

2. Materials and Methods

2.1. Regulatory Background

In the legislation of the EU, light-duty vehicles include passenger cars and light commercial vehicles, while heavy-duty vehicles include trucks and buses.

Originally emission regulations for light-duty vehicles were introduced in the 1970s with Directive 70/220/EEC (only CO and HC) [1,106]. In the years after, other pollutants were added, and various reductions of the emission limits were applied. In 2007 regulation 715/2007 defined Euro 5 and Euro 6 standards. The pollutants currently regulated are CO, HC (for positive ignition (PI) engines only), NO_x, HC + NO_x (only for compression ignition (CI) engines), particulate matter (PM), and particle number (PN) (only for CI and PI direct injection engines). CO_2 has limits only as fleet-average. The measurements were conducted mostly from bags that collect a sample from a dilution tunnel with constant volume sampling (CVS), where the whole exhaust gas was diluted.

In 2017, with Euro 6d-temp, additional on-road testing was added to the laboratory type approval and in-service conformity testing. Limits were defined only for PN and NO_x, while CO and CO_2 had to be measured. The limits were the laboratory type approval limits taking into account the additional measurement uncertainty of the on-board portable emissions measurement systems (PEMS) with temporary conformity factors [107,108]. Since 2020, with Euro 6d the revised conformity factors were applicable. Regulation (EU) 2018/858 introduced a new EU type-approval framework (from September 2020), with an effective market surveillance system to control the conformity of vehicles already in circulation (new In-Service Conformity process from September 2019).

Heavy-duty standards were originally introduced with Directive 88/77/EEC (applicable from 1992). Current Euro VI emission standards were introduced by Regulation 595/2009 followed by a number of amendments that specified technical details. Limits are applicable for CO, non-methane hydrocarbons (NMHC), CH_4 (for gas engines) NO_x, PM, PN, and NH_3. The measurements can be conducted from bags, directly from the full dilution tunnel, from a proportional partial flow system (PDFS), or directly from the tailpipe. Euro VI regulation introduced in-use testing with field measurement using PEMS. Conformity factors are applicable that take into account the additional measurement uncertainty of the PEMS.

At a global level, GTR 15 (global technical regulation) for light-duty vehicles includes additional pollutants (only methodology, not limits), and the EU is highly likely to adopt most of them in future regulations. None of these pollutants, however, are prescribed as candidates for on-board testing. Table 1 summarizes the pollutants, their principle of measurement and their inclusion or not in the current EU regulations. Some of them were recently introduced in other countries (e.g., N_2O in China 6, aldehydes in Brazil, Korea, USA) [109].

Based on Table 1, FTIR is permitted to be used for the measurement of NH_3, N_2O, C_2H_5OH, CH_2O, and CH_3CHO. However, with the current regulations, FTIR would have to be connected to the tailpipe for the measurement of NH_3, but at the dilution tunnel for the rest of the pollutants. As FTIR can determine simultaneously many of the regulated pollutants (CO_2, CO, NO, NO_2, CH_4), and has the capabilities to be used at the tailpipe (e.g., for NH_3), it is an attractive candidate for on-road testing.

Table 1. Pollutants, principle of measurement, and the sampling option for light-duty (LD) vehicles and heavy-duty (HD) engines in the European Union (EU) regulation and the global technical regulation (GTR 15) for LD vehicles. PEMS (portable emissions measurement systems) refer to the EU regulation for both LD and HD vehicles. Measurements can be conducted directly from the dilution tunnel with constant volume sampling (CVS), the bags, the proportional partial flow dilution system (PFDS), or the tailpipe (TP), depending on the regulation.

Compound	Measurement Principle	GTR15 (LD)	EU LD	EU HD	PEMS
PN	VPR + PNC	CVS	CVS	+PFDS	TP
PM	Gravimetric (filter)	CVS	CVS	+PFDS	
CO_2	NDIR	bags	bags	+CVS, +TP	TP
CO	NDIR	bags	bags	+CVS, +TP	TP [3]
THC	FID or HFID (for diesel)	bags	bags	+CVS, +TP	TP [3]
CH_4	NMC or GC combined with FID	bags	bags	+CVS, +TP	TP [3]
NMHC	Calculated (THC–CH_4)	(bags)	(bags)	calculated	TP [3]
NO_x	CLA or NDUV	bags	bags	+CVS, +TP	TP
NO	CLA or NDUV (only bags)	CVS or bags			
NO_2	NDUV, QCL (or CLA) or ($NO_{x,bags}$–NO_{CVS})	CVS			
N_2O	GC with ECD, QCL-IR, NDIR, FTIR [1]	CVS or bags			
NH_3	LDS or QCL or FTIR [2]	TP		TP [4]	
C_2H_5OH	Impinger + GC, FTIR, PAS, PTR-MS, dir. GC	CVS			
CH_2O	DNPH + HPLC, FTIR, PTR + MS	CVS			
CH_3CHO	DNPH + HPLC, FTIR, PTR + MS	CVS			

[1] interferences < 0.1 ppm; [2] with interference < 2 ppm at max CO_2 and H_2O; [3] only for heavy-duty vehicles; [4] LDS or FTIR for HD engines. C_2H_5OH = ethanol; CH_3CHO = acetaldehyde; CH_4 = methane; CLA = chemiluminescence analyzer; CO = carbon monoxide; CO_2 = carbon dioxide; DNPH = 2,4-Dinitrophenylhydrazine; ECD = electron-capture detection; FID = flame ionization detection; FTIR = Fourier transform infrared spectrometry; GC = gas chromatography; CH_2O = formaldehyde; HFID = heated flame ionization detection; HPLC = high-performance liquid chromatography; IR = infrared; LDS = laser diode spectrometer; N_2O = nitrous oxide; NDIR = non-dispersive infrared spectrometry; NDUV = non-dispersive ultra-violet spectrometry; NH_3 = ammonia; NMC = non-methane cutter; NMHC = non methane hydrocarbons; NO = nitrogen oxide; NO_2 = nitrogen dioxide; NO_x = nitrogen oxides; PAS = photoacoustic spectrometry; PM = particulate matter; PN = particle number; PNC = particle number counter; PTR-MS = proton transfer reaction—mass spectrometry; QCL = quantum cascade laser; THC = total hydrocarbons; VPR = volatile particle remover.

2.2. FTIR Description

FTIR can be used to measure substances (solids, liquids, gases, powders, polymers, organics, etc.) that absorb in the mid-infrared (i.e., approximately 400–4000 cm^{-1}). As a basic principle of the interaction matter–radiation, absorption can occur at intrinsic energy levels, specific for each molecule. When mid-infrared radiations cross a molecule, some specific frequencies (or wavelengths) will be absorbed if they correspond to the transition of vibrational levels of the molecule. Consequently, FTIR can be used for qualitative and quantitative analysis. However, it cannot detect noble gases, such as helium (He) and argon (Ar), or diatomic gases, such as oxygen (O_2), nitrogen (N_2), and hydrogen (H_2), as their vibration does not create a dipole moment, thus do not have absorbance bands in the infrared region of the electromagnetic spectrum. Others molecules absorb very little radiation and are, therefore, not detectable at low concentrations (e.g., H_2S > 200 ppm [110]).

The heart of every FTIR instrument is an optical device called an interferometer (Figure 1) [3]. The oldest and most common type is the Michelson interferometer. The infrared source is usually a heated ceramic (at ca. 1200 °C). A collimating mirror collects light from the source and makes its rays parallel. A beamsplitter (in KBr) transmits approximately half of the light incident upon it and reflects the remaining half. A fraction of the light transmitted travels to a fixed mirror, while the other fraction travels to a moving mirror (see Figure 1). The lights are reflected by the two mirrors back to the beamsplitter, where they are recombined into a single light beam. This light beam interacts with the sample (exhaust gas) in a gas cell and finally strikes the detector. A multireflection cell is used to obtain a long optical path length with the minimum possible volume of the cell [111].
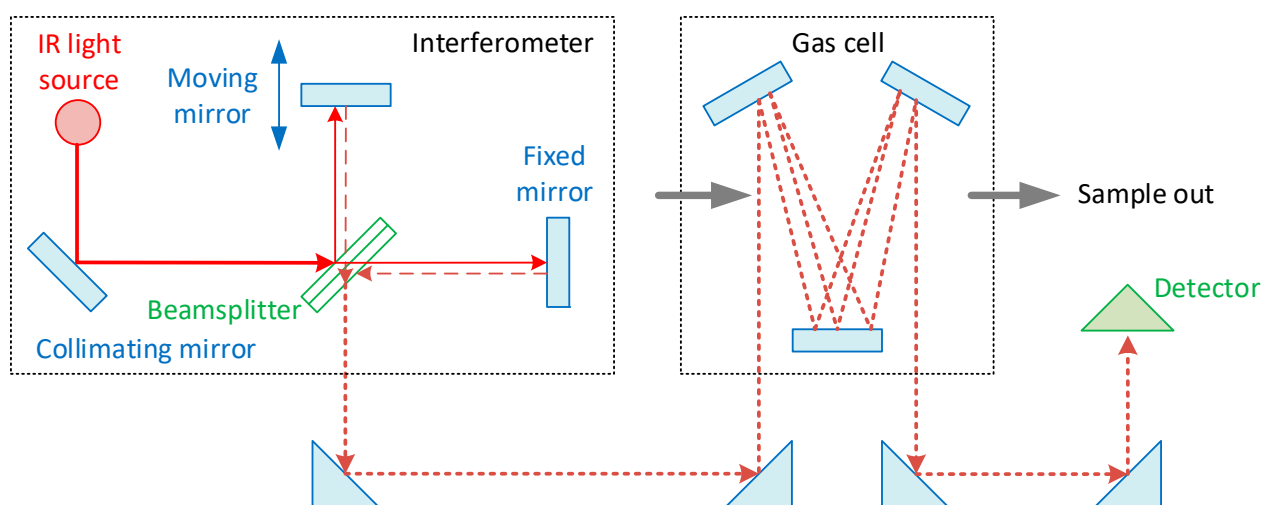
Figure 1. Principle of operation of FTIR (Fourier transform infrared) spectroscopy. IR = infrared.

Because the path that one beam travels is a fixed length and the other is constantly changing as its mirror moves, the signal which exits the interferometer is the result of these two beams "interfering" with each other. The resulting signal is called an interferogram (i.e., a plot of light intensity versus optical path difference). The interferograms measured are then Fourier transformed to yield a spectrum (i.e., a plot intensity versus frequency/wavenumber).

There is also a laser (not shown in the figure) whose light follows the infrared beam. This laser light is used to measure the optical path difference of the interferometer. The spectral resolution (in cm^{-1}) depends on the inverse of the optical path difference. This gives the wavelength accuracy (or Connes' advantage) compared to dispersive instruments where the scale depends on the mechanical movement of diffraction gratings. Thus, the FTIR can give very accurate frequencies in the spectrum—this enables processing techniques such as spectral subtraction. It was shown that for automotive applications, a resolution of 0.5 cm^{-1} is the best compromise to obtain suitable fineness of the spectra (required to build robust calibration method) without compromising signal to noise ratio [8]. At lower resolutions (e.g., 1 cm^{-1}), water's absorbance bands may create interference problems that affect the detection limits of many compounds [112]. The accuracy and detection limits of the individual compounds measured are dependent on the intensity of the respective absorbance bands and their interference, but also on the detector [113,114]. For most compounds, the detection limit is well below 1 ppm for 1 s resolution [55,115]. The resolution of 0.5 cm^{-1} is achievable only with a photonic detector (e.g., Mercury Cadmium Telluride—MCT) that needs to be cooled down with liquid N_2. Peltier cooled MCT or heating detector (e.g., Deuterated TriGlycide Sulfate—DTG)) are less sensitive and reactive compared to photonic detectors. However, they might be more suitable for portable systems. Another advantage of the FTIR is the multiplex advantage (or Fellgett advantage) because all wavelengths are collected simultaneously and thus a spectrum can be obtained very quickly. In contrast, with "dispersive spectroscopy" a monochromatic light beam shines at a sample, the absorbed light is measured, and this is repeated for each different wavelength. The throughput advantage (or the Jacquinot advantage) arises because, unlike dispersive spectrometers, FTIR spectrometers have no slits, which attenuate the infrared light, resulting in a higher signal-to-noise ratio.

Other advantages of the FTIR systems are: measurement of many pollutants simultaneously, real-time operation, possibility to measure undiluted exhaust gas, the fast response time (at least as fast as the conventional analyzers) for transient engine operation, low minimum detection limits, large dynamic range for dilute and direct sampling, high accuracy with negligible cross-sensitivity [31]. On the other hand, the interference primarily from H_2O and CO_2 can be high, and the signal-to-noise ratio can be affected by external vibra-

tions. Figure 2a plots absorbance of CO and different nitrogen compounds (lower part), and CO_2 and H_2O (upper part) in arbitrary scales for better visualization. The example is based on the reference library acquired with a HR-FTIR MKS Multigas analyzer 2030 (Andover, MA, USA) at 191 °C, 0.95 atm and with a 5.11 m optical path measurement cell. Such reference spectra can be found from instrument manufacturers or from the Hitran (Cambridge, MA, USA) database [116,117]. It is evident that there are areas with overlap (e.g., NO_2, NH_3 and H_2O). CO_2 measurement is relatively straightforward, but the selection of the bands needs to be conducted considering H_2O interference, and between CO absorbance peaks. CO requires the careful selection of infrared absorbance bands to stay within the desired absorbance range and in an area between H_2O and potential N_2O absorption region. NO and NO_2 absorb only in regions with very high levels of water interference, as well as CO and CO_2 interferences. Thus, for these compounds, the selection of the absorption bands needs to be conducted between, e.g., H_2O absorption peaks, in the area between ca. 1850 and 1940 cm^{-1} for NO, and between 1570 and 1650 cm^{-1} for NO_2. Figure 2b provides the example of NH_3 calibration method, for which a rather straightforward selection of the absorption bands is possible within an area where no interference is expected (between 900 and 970 cm^{-1}). Figure 2c provides the example of the N_2O, for which the absorption bands need to be selected in an area located outside the CO_2 absorption range, and between the CO absorption peaks. More detailed discussion on spectral regions for the analysis and interferences can be found in the literature [28,47,104,118,119]. Estimations of cross-sensitivities simulating exhaust gas gave an influence of <<1% for most compounds (NO_2, CO, NH_3) [114], but >1% for acetaldehyde (CH_3CHO), acetone (CH_3COCH_3), C_6H_6, and C_7H_8, because their absorption spectrums are not sharp and strong, and/or the region of possible quantification is small due to the co-existing components. The actual interference might be different if there are interfering compounds not included in the software, if some wavelengths are saturated due to high concentrations, and/or the resolution is not enough to resolve the species, e.g., water, NO, NO_2, and NH_3 [120].

(a)

Figure 2. *Cont.*

(b)

(c)
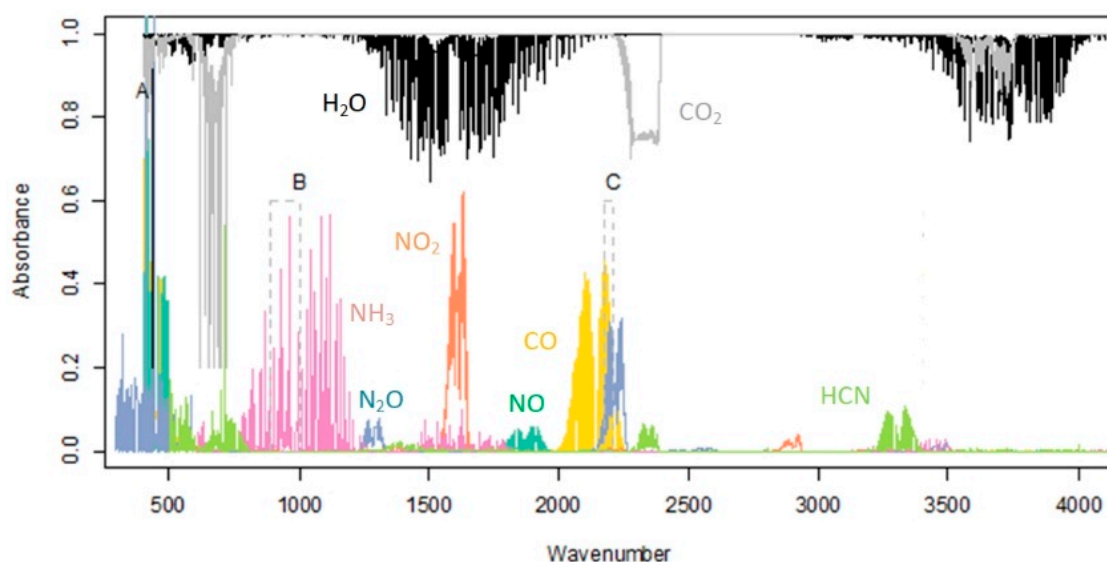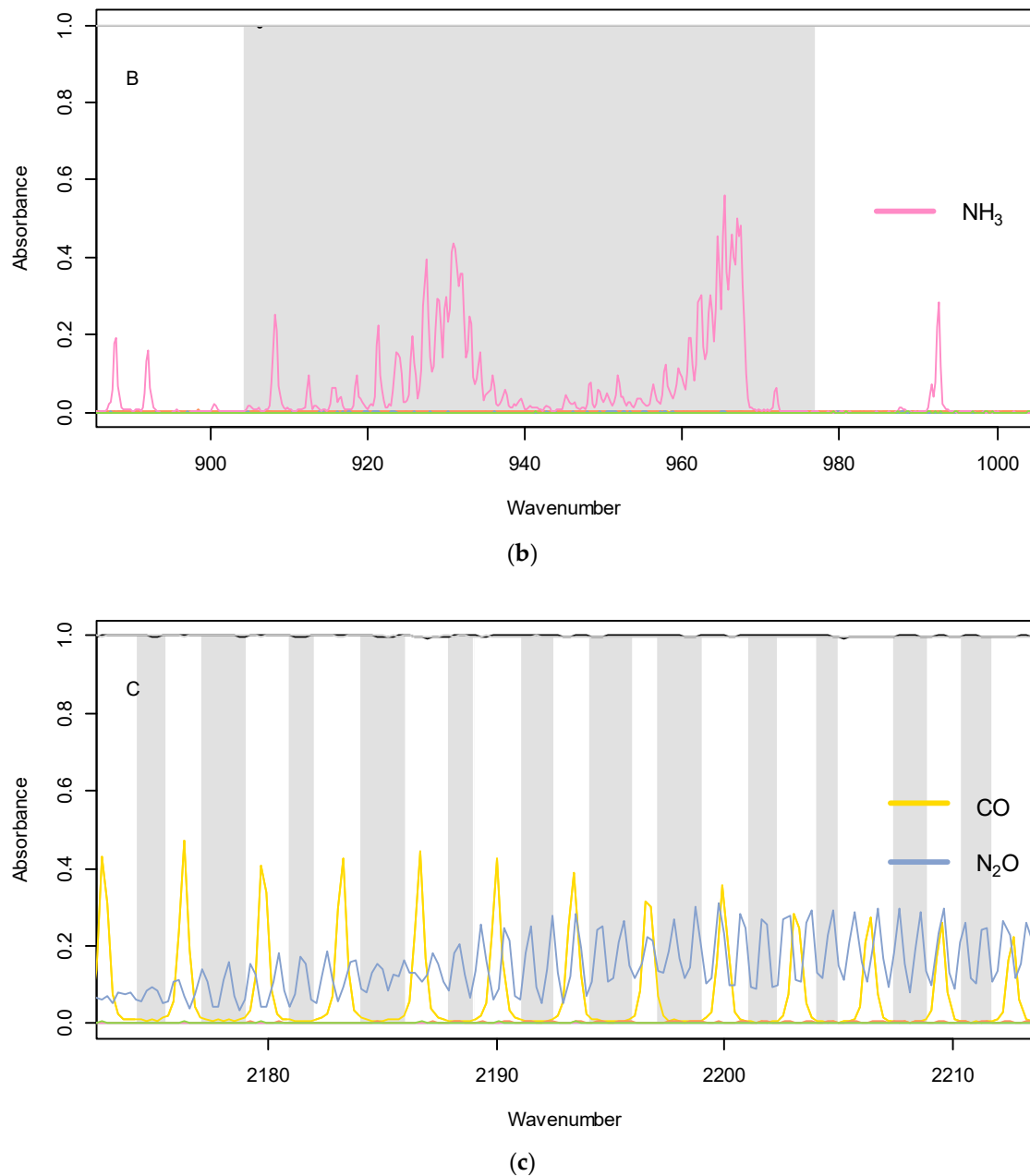
Figure 2. Example of absorbance versus wavenumbers: (**a**) for various species with concentrations of 398 ppm (CO), 97 ppm (NO), 136 ppm (NO_2), 93 ppm (N_2O), 93 ppm (NH_3), 0.8% (CO_2), 2.03% (H_2O). For better visualization, the spectra of H_2O and CO_2 were reduced by a factor of 10 and displayed in an inverted axis. For the same reason, NH_3 and HCN spectra were increased by a factor of 2 and 4, respectively; (**b**) NH_3, area B of panel (**a**); (**c**) N_2O, area C of panel (**a**).

Principally, transmission-FTIR spectroscopy follows the Lambert–Beer law. Consequently, for a given optical path length, a linear relationship between the compound concentration and the absorbance mediated by this compound can be assumed. However, the output voltage of the detector is not a linear function of the incident radiation power [121] and non-linearity can be seen for components such as CO_2, H_2O, CO, and NO_x with a wide range of variations [8]. Thus, for some components, the calibration might not be a linear function, but quadratic, cubic, etc. Because the mirror travels only a finite distance, the interferogram is truncated, and the Fourier transform results in a spectrum with broader features and spurious oscillations at the wings of the features. An apodization function is applied to reduce the magnitude of these oscillations but further broadens the spectral features. This broadening causes the instrument to have a nonlinear response to

changes in absorption of the various gases being measured [122]. This can be modeled and corrected.

FTIR requires no daily calibration per se. This is possible because the daily background/zero scan is compared point per point to the measurement spectrum and compensates for any instrument drift in the final absorbance spectrum. Since the same number of molecules always absorb the same fraction of incident energy (independent of the total amount of energy), the calibration factor remains the same for a given compound and wavenumber and as a result there is no span drift or calibration drift [115]. However, since background and measurement spectrums are acquired successively, the FTIR needs to be very stable, in terms of infrared source, detectors, but also in terms of composition of the gas included in the instrument. Such stability is insured by keeping the instrument always on (heated), and by purging the optical system with dry gaseous N_2.

The sampling lines and the sampling cell for exhaust gas application need to be heated above 100 °C (usually 191 °C) to avoid water condensation, which would lead to an underestimation of the hygroscopic compounds (e.g., NH_3). In addition, the sampling line located upstream is usually equipped with a heated filter that prevents the deposition of particles on the mirrors' surface of the multipath gas cell, and thus, the modification of the optical path length.

2.3. Processing of the Interferogram

The interferogram produced by the interferometer is converted mathematically (Fourier transform) into an intensity versus wavenumber plot known as a single-beam spectrum (Figure 3). The single-beam spectrum of the gas exhaust sample is ratioed (logarithmically) against the single-beam background spectrum (produced by passing nitrogen gas through the cell) to produce the absorbance spectrum [123]. Other processing of raw data (apodization) may be used to smoothen discontinuities at the beginning and end of the spectra, reduce, or eliminate noise [3,124].
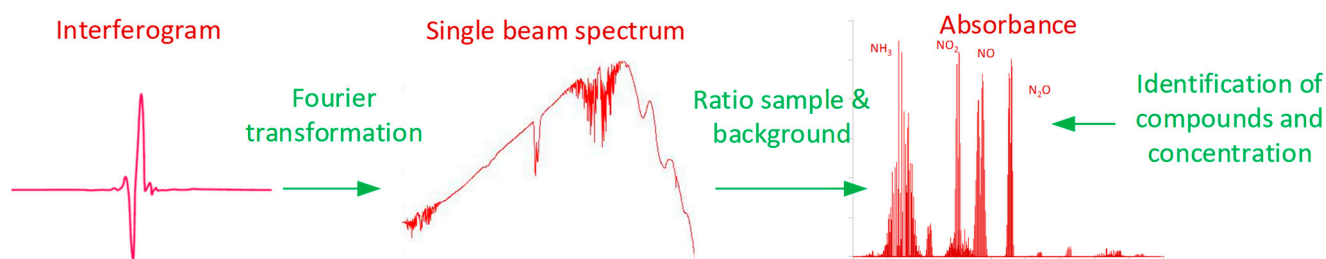
Figure 3. Processing of an interferogram.

Then, to utilize the complete information of the complex spectra and to handle the large data set, multivariate analysis is often used (i.e., data analytical methods that deal with more than one variable at a time). Some combinations of variables (wavenumbers) of a given data set are highly correlated with each other. Principal component analysis (PCA) is one such widely used dimensionality reduction technique to extract the informative region of the spectra for every individual species. Unlike classification or clustering, regression is used in the quantification of particular dependent variables (expected pollutants). Some of the commonly used multivariant regression methods are classical least squares (CLS), multiple linear regression (MLR), principal component regression (PCR), partial least squares (PLS) [125]. Such calibration methods can be appropriate when the gas composition of the mixture to be analyzed (here, the exhaust gas) is not known. In that case, the compound of interest can be added to the mixture (matrix) at different concentration levels (spiking) in order to build a suitable multivariate regression model. This model might, however, highly depends on the complexity and composition of the gas mixture (matrix) used to build it.

Another approach is to compare the spectra of the compound of interest to the foreseen interfering compounds (e.g., water or CO_2) in order to: (i) identify the wavelength region

where not too many interferences are expected, and (ii) identify the other wavelength regions where interferences are expected. The first region is then used to build the regression model, sometime in a straightforward way (see Figure 2b), or less straightforward way (see Figure 2c). The second set of wavelength regions will be used to foresee the possible interference brought by the compound of interest when building a regression model for other compounds. For illustration, Figure 2c shows how the N_2O model is built in a wavelength area where the possible interference of CO absorption was identified. In this case, the region used to build the regression model was selected to avoid the interference of CO_2 and H_2O (see Figure 2a). Typically, specific wavelengths where no other species absorb are used to predict the volume concentration of the compound, assuming a linear or quadratic relationship between concentration and absorption [28,47,118]. For each compound, standard gas cylinders of several concentration levels are used to calibrate the model. Such an approach has the advantage of being more robust and less dependent on the composition of the mixture. However, this approach requires to be exhaustive in consideration of the expected interferences, thus having a library including the pure spectra of all the compounds expected to be found in vehicle exhaust.

Once the regression model is built, analysis of the spectral residual is also a crucial step in order to identify potential interfering compounds in the models created. It is important to highlight that the reference spectra must be recorded at the same conditions, meaning the same instrument (same optical system, including optical path), and same temperature and pressure as used for the exhaust measurements [126,127]. The processing of the data is not standardized, but FTIR data can be re-processed differently with a different method to reveal the concentration data of other components. It is important to mention that FTIR is a non-destructive measurement technique. Thus, it could be possible to direct the analyzed gaseous sample toward another measuring instrument for complementary analysis. It should be, however, recalled that the sampling gas is heated (e.g., 191 °C) and filtered.

3. Results

The following sections summarize the results of the studies that assessed FTIRs against calibration gases or reference instruments. The sections present shortly the principle of operation of the reference instruments (details can be found elsewhere, e.g., [128–130]) and any advantages and disadvantages over FTIR. Then the results of the studies that have assessed FTIRs are summarized. The details of the studies can be found in the Appendix A. Each table gives first the results with calibration gases. Then, the comparison of the FTIR and reference analyzers is divided into cases that both instruments were at the same location (dilution tunnel or tailpipe), or different (FTIR at tailpipe, reference at dilution tunnel). In the last case, the differences can be affected significantly by the uncertainty of the exhaust flow determination.

To put the assessed values into perspective, Table 2 presents Euro 6/VI limits for light-duty vehicles and heavy-duty engines, an approximation of the mass emissions of 1 ppm concentration of various pollutants. Exhaust flows of 2 kg/km and 10 kg/kWh were assumed as the highest values for large engine displacement light-duty vehicles and heavy-duty engines [103]. The density ratios u of the relevant regulations were used.

Table 2. Current Euro 6/VI limits in the laboratory (min from compression ignition and positive ignition engines) for light-duty (LD) vehicles and heavy-duty (HD) engines. The uncertainty of 1 ppm is also expressed in mass considering exhaust flow of 2 kg/m^3 for LD and 10 kg/m^3 (HD) large engine displacement vehicles.

Pollutant	CO	NO$_x$	HC	NH$_3$	N$_2$O
Euro 6 limits (min of LD) [mg/km]	500	60	100	-	-
1 ppm uncertainty (LD) [mg/km]	1.9	3.2	1.0	1.2	3.0
Euro VI limits (min of HD) [mg/kWh]	4000	460	660	10 ppm	-
1 ppm uncertainty (HD) [mg/kWh]	9.7	15.9	4.8	5.9	15.2

3.1. Carbon Monoxide (CO) and Carbon Dioxide (CO$_2$)

CO and CO$_2$ are typically measured with NDIR (Non-Dispersive Infrared) absorption type detectors. NDIR is one of the IR methods, which is not spectroscopic analysis but uses non-dispersive infrared light. In NDIR, the region of wavelengths used for analyzing the target component is selected by using an optical filter (multilayer interference filter) or a gas filter (a cell enclosing interfering gases). Other gases that show absorption in the same wavelength region will contribute to the measurement result of the target component. For example, when analyzing CO in the engine exhaust gas, CO$_2$ and H$_2$O also included in engine exhaust gas are likely to interfere with the measured CO concentration [131]. The CO NDIR analyzer may require a sample conditioning column containing CaSO4, or indicating silica gel to remove water vapor, and containing ascarite to remove carbon dioxide from the CO analysis stream (USA EPA Title 40, Chapter I, Subchapter C, Part 86, Subpart B, §86.111-94). Many analyzers use coolers. The regulation requires interference checks of the CO analyzer with CO$_2$ and H$_2$O at concentrations expected during the tests. The CO response has to be within 2% or ±50 ppm (whichever is larger). For analyzers measuring from the dilution tunnel, the allowed interference is between −1 ppm to 3 ppm. Regarding CO$_2$ measurements of diluted exhaust, the regulation requires that the CO$_2$ concentration in the dilute exhaust sample bag is <3% for gasoline and diesel engines, <2.2% for LPG engines, and <1.5% for natural gas and biomethane engines. When the concertation of water is <3% H$_2$O the error is <1% [132].

For tailpipe sampling, in order to minimize the interference for non-diluted exhaust, additional detectors sensitive only to the interfering component can be added [133], or the H$_2$O can be removed (e.g., by a cooler) [134]. Errors after corrections with additional H$_2$O detector, the main interfering component in the exhaust gas, are <2% for H$_2$O concentration up to 12% [133]. Removal of the water needs a dry-to-wet correction, which has a low error, as long as no condensation takes place at the sampling lines, e.g., at cold start. In such cases errors of up to 10% have been reported during the cold start period [135].

Table A1 summarizes the studies assessing FTIR CO$_2$ readings with calibration cylinders or NDIR analyzers. Table A2 summarizes for CO. Regarding CO$_2$, in most cases, the differences were within ±5% (slope 0.95–1.05), with only a few exceptions that the differences were around 10%. There were no particular differences between gasoline or diesel vehicles. The correlation coefficient was high (>0.95). The only exception (R^2 = 0.70, FTIR at tailpipe vs. dilution tunnel) was when a calculated from the intake air exhaust flow was used instead of measured with exhaust flow meter. Higher differences (−21%) were reported when the response of the FTIR was slow [34].

Regarding CO, the mean differences were within ± 5% of the reference analyzers, but the scatter was very high in some cases, exceeding 50%. The slopes were within 0.8 and 1.2 with no indications of higher slopes when the FTIR connected at the tailpipe was compared to the dilution tunnel or bags. The worse performance of the FTIR CO compared to the CO$_2$ might have to do with the higher interference of water and CO$_2$, and the higher concentration range of CO compared to the CO$_2$.

3.2. Nitrogen Monoxide (NO) and Nitrogen Dioxide (NO$_2$)

NO and NO$_x$ (sum of NO and NO$_2$) are typically measured with chemiluminescence analyzers (CLA) developed in early 1970s [120]. NO reacts with O$_3$ and the excited NO$_2$ molecules spontaneously return to normal state emitting light (chemiluminescence) [136]. The sensitivity for NO is influenced by the existence of CO$_2$ or H$_2$O in the sample gas, because the excited NO$_2$ can react with CO$_2$ and H$_2$O (quenching effect) [128]. The effect is <1%, in particular for systems with H$_2$O sensors that can compensate for H$_2$O concentrations up to 14% [137]. The light can also be filtered before being measured by the photomultiplier to minimize interference [130].

The CLA can be used to measure NO$_x$. In this case, a carbon or active metal-based furnace converts NO$_2$ into NO (NO$_x$ converter) [120,136]. Regulations require a conversion efficiency of >95%. However, NH$_3$ can also be converted to NO in the converter. The

conversion efficiency depends on the converter material, the temperature and the concentrations of NO and NH_3. With a 5:1 ratio of NH_3 to NO, an error of 30% was estimated for NO_x [120]. Nevertheless, laboratory CLA today has a cross-sensitivity of <1 ppm for 1000 ppm NH_3. NH_3 could also cause a loss of conversion efficiency of the NO_x converter over time. On the other hand, NO_x can be converted to N_2 or NH_4NO_3 (ammonium nitrate), resulting in a lower concentration [120]. Ammonium nitrate formation is very rapid even at room temperature if NH_3 and HNO_3 are present. HNO_3, in turn, is readily formed when NO_2 dissolves in liquid water. Ammonia scrubbers can be used to avoid this problem with CLA [138]. The disadvantages over FTIR are the extra expenses required for an ozonizer, NO_2 to NO converter with converter efficiencies >95% (which need to be checked every month according to EU Regulation), possible NO_2 losses in the chiller, influence due to quenching from water and CO_2 [136,139]. FTIR was also found to provide accurate measurements of NO_x in the presence of NH_3 [120].

Table A3 summarizes the studies that the FTIR NO_x reading was compared to calibration cylinders or CLA. The comparisons with calibration gases were within $\pm5\%$, while with reference CLA within $\pm10\%$, with a few exceptions. For example, a study had 30% difference due to different exhaust flows used for the FTIR and the PEMS [110]. Higher differences were reported when the response of the FTIR was slow [34]. Comparison of tailpipe FTIR with dilution tunnel bags were also within $\pm10\%$, with only a few exceptions. In some cases, the laboratory analyzers were suspected [98].

The comparisons of FTIR and CLA for NO_2 did not always give acceptable differences, with differences exceeding 10% in particular at different sampling locations [140]. One explanation might be due to the fact that NO_2 is not directly measured but calculated from the difference between NO_x and NO. Wrong CLA NO_2 measurements can also originate from different time delays in the analyzer for NO and NO_x [141], and as mentioned before, converter-related side reactions. Partly lower NO_2 concentrations peaks due to reaction of NO_2 with soot contamination have also been reported [141]. Finally, despite the advantages of FTIR spectroscopy, the fundamental interference of NO_2 measurement by water vapor remains. It should be added that NO_2 (and NH_3) are considered "sticky" substances and the sampling setup is very important. NO_2 can be underestimated if it adsorbs on surfaces in the sampling system, dissolves in the condensed water [142], or forms a salt in the presence of NH_3 and remains in the sampling filter. Chiller penetration is defined in the USA regulation for analyzers that do not use NO_2 to NO converter upstream of the chiller. Heated CLA systems are used when high NO_2 concentrations are expected in order to avoid the loss of water-soluble NO_2 inside the dehumidifier. The dry-to-wet correction introduces an uncertainty, which is significant during cold start [135]. Lower NO_2 concentrations peaks over test cycle as reaction of NO_2 with soot contamination have been reported [141].

All reference instruments presented in the table applied the CLA principle. Only in one case the reference instrument was a PEMS applying the NDUV principle [102]. The NDUV measurement method is based on the absorption of ultraviolet (UV) radiation from a broadband UV source to quantify the amount of NO_x in a given sample [139,143]. The NO and NO_2 signal occurs during the very large water wavelength in addition to other smaller contributing signals such as sulfur compounds [144]. For this reason, the sample is typically dried. The portable FTIR and the NDUV analyzer agreed well (slope 1.03, R^2 0.97) [102]. This was expected as NDUV and CLA usually agree. For example, a study found the two principles within 5% for 20–130 ppm concentrations [145].

3.3. Nitrous Oxide (N_2O)

Nitrous oxide (N_2O) can be measured using FTIR, NDIR, QCL-IR, and GC with ECD. One study [102] compared two FTIRs measuring the tailpipe exhaust of diesel vehicle and found a slope of 0.96 ($R^2 = 0.95$) for concentrations up to 60 ppm. Another study compared the FTIR reading from bags with exhaust gas injected with N_2O and found differences

within 3% of the expected values [146], indicating no particular interference from H_2O or other exhaust gas components.

3.4. Ammonia (NH_3)

Ammonia can be measured using FTIR, QCL or LDS from the tailpipe.

A Quantum Cascade Laser (QCL) element emits an intermittent mid-infrared laser beam in a sample cell at a very specific wave number by applying a pulsed current [128,147,148]. During a pulse, the element temperature varies, and, consequently, the actual wave number continuously shifts within a narrow range. Compounds that absorb energy in this oscillation range will decrease the light intensity and will be detected at the relevant wave numbers.

The measurement principle of a Laser Diode Spectrometer (LDS) is based on single line molecular absorption spectroscopy [149]. A diode laser is used for emitting a near-infrared (compared to QCL mid-infrared) light beam through the sample gas, and the light is detected by a receiver. The laser diode output is tuned for a gas-specific absorption line. Cross-sensitivities of the method is insignificant as, spectrally, the laser light is much narrower than the gas absorption line.

Table A4 summarizes the studies that FTIR was assessed in measuring NH_3. The calibration gases readings were within 5% of the specified values. In general, the agreement between FTIRs was good. Steady-state engine tests with NH_3 dosing showed the importance of the FTIR response time and the sampling line conditioning. The differences in dynamic response indicated buffering of NH_3 (known to "stick" on walls) within the sampling line before breakthrough to the analyzer cell [150].

The comparison of FTIRs with QCLs was also good on average. In one case, examining real-time graphs, higher and sharper peaks were obtained with the QCL due to the 10-Hz frequency [151]. Comparison of an FTIR with chemical ionization mass spectrometry (CI-MS) gave good agreement [152], and comparisons with an in-situ (cross-duct, without sampling line) LDS was also in good agreement [149].

There were only a few studies comparing tailpipe with dilution tunnel [152,153]. However, as pointed out by these studies, severe losses of ammonia can occur in the dilution tunnel resulting in lower emissions.

The sampling location and the sampling conditions are very important for NH_3 measurements. As it was mentioned in the NO_x section, the formation of ammonium nitrate is also possible in the presence of HNO_3. Low sample line temperature can result in condensation inside the heated line, which can lead to loss of NH_3. On the other hand, upstream of the SCR in the presence of HNCO and H_2O, a high sample line temperature can produce NH_3 [150]. For such cases, a temperature of 113 °C was recommended. Downstream of the SCR, no such phenomena were observed.

3.5. Hydrocarbons (HCs) and Methane (CH_4)

Total hydrocarbons (THC) and methane (CH_4) are typically measured with Flame Ionization Detection (FID). In FID, the sample gas is introduced into a hydrogen flame, where some of the HCs in the sample gas are ionized [154,155]. Due to the ions, an electric current is generated at the applied electric potential, is nearly proportional to the amount of carbon atoms. For this reason, the HCs concentration is called "THC" and the unit is "ppmC". A heated FID should be used in applications such as diesel exhaust that contains significant quantities of high boiling point HCs to avoid condensation and loss of heavier HCs [128]. The FID detector temperature should be set to 113 °C for alcohol-fueled vehicles (instead of 190 °C, which is used for diesel-fueled vehicles) (USA EPA Title 40, Chapter I, Subchapter C, Part 86, Subpart B, §86.111–94). This is based on the higher water vapor of methanol and the fact that methanol can undergo decomposition reactions if the oven is too hot [156].

The FID sensitivity for each HC is represented by a "response factor" that indicates the relative sensitivity compared to propane as the calibration gas. Generally, the FID has

lower sensitivity to oxygenated HC components such as alcohols, aldehydes [157–160] and no sensitivity to formaldehyde. For regulatory purposes, FIDs are calibrated to have a response factor of 1 for propane. Toluene and propylene have to be within 0.9 and 1.1. The FID has negligible interference from inorganic components such as CO, CO_2, H_2O, and NO, except for O_2 in the sample gas. The O_2 concentration in the sample can affect not only FID sensitivity for HCs but also the zero point. Some THC analyzers have a compensation function for O_2 interference using an additional O_2 analyzer. The regulation allows a maximum of 1.5% oxygen interference.

For measuring CH_4 in the engine exhaust gas with the FID analyzer, sample conditioning parts, i.e., Gas Chromatography (GC) or Non-Methane Cutter (NMC), are placed before the detector to extract or separate CH_4 from the other HC components. The GC-FID-based CH_4 analyzer is only suitable for batch measurement rather than continuous measurements. A Non-Methane Cutter (NMC) is a catalyst that selectively oxidizes HCs and only minimally CH_4. The regulation requires the determination of the methane conversion efficiency, which ideally should be 0%, and the ethane conversion as an approximation of the conversion efficiency of the non-methane hydrocarbons, which should be >98%. If the CH_4 response is <1.05, it may be omitted from the calculations of the emissions.

Non-Methane Hydrocarbons (NMHCs) are calculated as the difference of THC and CH_4. (details in regulation, it is not a simple subtraction as conversion efficiencies need to be considered). In EU for high ethanol content fuels a different density is used to calculate THCs and NMHCs (0.934 g/L E85 vs. 0.646 g/L E10). In USA, non-methane organic gases (NMOG) include NMHCs, alcohols and carbonyls. Therefore, to measure NMOG (gasoline with ethanol > 25%), one must separately measure the principle alcohols, aldehydes, and ketones, subtract their inaccurate contribution to the FID signal, and add in their correct concentrations. Ethanol is traditionally measured by impinger collection and GC. Alternatively, the ethanol levels in diluted emissions sampled into Tedlar bags can be read directly via a photoacoustic non-dispersive infrared method [161], thus avoiding the need for off-line impinge analysis. Aldehyde measurement is via DNPH cartridge collection and off-line high-pressure liquid chromatography. Thus, ethanol and acetaldehyde are measured via batch methods, thus precluding time-resolved NMOG data.

FTIR spectroscopy provides an attractive alternative because all of the species contributing to NMOG are infrared active. For FTIR, in general, the analysis of infrared spectra works best for components with strong and sharp absorbance bands [113]. It is progressively more difficult for FTIR to speciate hydrocarbons as the number of carbons increases for two reasons [162]: (i) the individual molecular rotation-vibration lines coalesce into broader bandshapes. (ii) they progressively overlap with each other.

Table A5 summarizes the comparisons of FTIR with FID systems for THC. There is a high scatter of the results. The differences are typically within 15%, but underestimation by a factor of 2 has also been reported [110,163]. Another study found FTIR measuring 34% higher than the FID from the dilution tunnel [164]. The explanation was the reduced sensitivity of FID to methanol and formaldehyde. It should be emphasized that this is a comparison of two technics, which are both estimating THC. None of them are specifically quantifying every single HC. FID is non-specific, and FTIR is non-exhaustive.

Table A6 summarizes the FTIR studies with CH_4. The differences were around 5% when measuring calibration gases and 10% compared to FIDs with NMC when measuring CH_4 from the tailpipe. The difference to other methods (GS) was within 5%. A few older studies found higher differences (up to 18%) at levels of <10 ppm CH_4. To put results into perspective of those older studies, when the FTIR was used at the tailpipe and then to measure the CH_4 from the bags, the differences remained the same (slope 0.88 and R^2 0.96) [165], indicating uncertainties with the FTIR. Similarly, a study that measured CH_4 from cylinders found a 3.5 ppm offset due to interference from other gases [166]. The same study found more than double emissions compared to chemical ionization mass spectrometry (CI-MS).

Table A7 summarizes the FTIR studies with NMHC. The differences were around 5%, with some cases having >30% differences. For these cases, an uncertainty analysis revealed that the most likely reason for the differences was the reference method. The reference method uncertainty was around 80–100 ppm (almost 50–100%), while for FTIR was around 25 ppm (10–15%) [162]. Another study, even assuming ethane and ethylene to have an error of 10% and the other components to have an error of 50%, found that the FTIR had a lower absolute error than FID for NMHC [167].

A promising proposal to measure real-time NMHC and NMOG with FTIR is to use a group of HCs, as a surrogate to NHMC and then combined it with ethanol, acetaldehyde and formaldehyde to calculate NMOG [162]. That study also showed that typically the top five organic compounds account for about 60% of the HC emissions with CH_4 the most abundant, and the top 10 compounds account for 80% for fuels ranging from gasoline to 85% ethanol/gasoline blends. The same study concluded that FTIR can measure NMHC and NMOG within 5% to the regulatory method [162].

Only a few studies compared ethanol emissions from FTIR and other methods. In one study, the differences were <10% for emission levels ranging from 100–1000 mg/km [160]. Another study with three FTIRs found on average −7% (0% to −12%) compared to PTR-Qi-ToF-MS during the cold start phase (emissions 150 mg/km) [168].

Regarding methanol many studies in the 1990s gave good results: slopes 0.72–1.10 (FTIR vs. impinger + CS) [26,112,169–171]. One study compared alcohols and found an agreement of 22% (FTIR vs. impinger + CS) for emission levels up to 250 mg/km and fuels up to E100 [172].

3.6. Formaldehyde (CH_2O) and Acetaldehyde (CH_3CHO)

The accepted techniques for measuring formaldehyde and acetaldehyde are DNPH + HPLC, FTIR, and PTR + MS; all from the dilution tunnel. The most common and cheaper method is using HPLC (high-performance liquid chromatography) to separate and quantify the carbonyls after extraction of 2,4-DNPH (dinitrophenylhydrazine) cartridges [173,174], while PTR-MS (proton transfer reaction—mass spectrometry) [168] is the least common. The DNPH-HPLC method also has its uncertainties, as the quantification by HPLC is not always straightforward due to the chromatogram peak resolution. NO_2, NO, and CO can have an impact on the quantification of formaldehyde and acetaldehyde due to the consumption of the DNPH during sampling [175].

Table A8 summarizes the studies that assessed the FTIR measuring formaldehyde. Sampling from the dilution tunnel showed in general good agreement with the DNPH + HPLC methodology (slopes close to 1), with one exception where the FTIR was on average 20–25% higher. From the tailpipe, the differences were larger (±30%).

Table A9 summarizes the studies that assessed the FTIR measuring acetaldehyde. The scatter of the results is high. One study found more than double concentrations of acetaldehyde with the FTIR than with the DNPH + HPLC method. It seems that the reaction of acetaldehyde took place in the exhaust pipe [176]. Another study with a flexi-fuel vehicle found 30% higher concentrations with the FTIR (compared to DNPH-HPLC), but at the same study, the FTIR was 30% lower than the PTR-MS method [168]. The emission levels were around 0.4 mg/km. Other studies found differences within 10%. A study that checked the FTIR formaldehyde concentrations according to analyte spiking EPA method 301 on a coal-fired burner found differences on the order of 10% [177]. The same study found 5% differences for acetaldehyde.

3.7. Other Compounds

A few only studies assessed alkanes. For example, differences from propane (C_3H_8) gas cylinders were 3.3% at 3200 ppm [95], and 13% at 2 ppm or lower concentrations. One ppm interference from CO_2 and/or H_2O was found at 15 ppm levels [178]. Ethane was measured 5–10% lower [166].

Isocyanic acid (HCNO) was assessed in one study for SCR (selective catalytic reduction for NO_x) applications with a heavy-duty diesel engine, and all three FTIRs were within a few ppm for concentrations up to 15 ppm [150].

Aromatic hydrocarbons (benzene, toluene) from FTIR were compared to the analysis of bags after Tenax TA adsorption and GC-MS analysis. Benzene was from −6.5% to +1.5% from bags for various fuels (gasoline, ethanol, methanol) [179]. The emission levels were around 2.5 mg/km, and the peaks at the cold start were around 20–30 ppm. The same study found differences of −3.5% to 2.4% (spike 40–60 ppm, emissions 7.5 mg/km) for toluene.

A very good correlation has been found for propylene, ethylene, acetylene, and benzene [180]. Results from other gases such as ethane, ethyne, 1,3-butadiene [166], acetylene, propene [113,171,181,182] can be found in the literature.

4. Discussion

FTIR analysis is seeing increased use in engine exhaust measurements. Since the first prototype instruments in the 1980s, many laboratories use FTIRs as a standard technique for engine development (see introduction). This review summarized the differences between FTIR and other methods for various gaseous components of engine exhaust. The differences were in most cases at acceptable levels (5–10%), but in some cases and for some compounds, higher differences were noticed. The main question is whether FTIR can be used for on-road regulatory purposes. To answer this question, the following topics need some analysis:

- Can FTIR measure undiluted exhaust accurately enough?
- Can FTIR be used on-board?
- How the FTIR accuracy can be ensured for regulatory purposes?

4.1. Tailpipe Applications

Interestingly, GTR 15 allows the use of FTIR for ethanol, formaldehyde, acetaldehyde, and N_2O only from the dilution tunnel. This is because there is no exhaust gas measurement to determine the emissions from the tailpipe. Only NH_3 has to be measured from the tailpipe. At the moment, there is a limit only for heavy-duty engines (in ppm) in the EU regulation (not in GTR). Such specifications would need two FTIRs for the measurement of non-regulated pollutants (e.g., one for NH_3 at the tailpipe and one at the dilution tunnel for the other pollutants). Permitting measurement of all pollutants from the tailpipe would simplify the setup. Furthermore, FTIR could be used instead of other analyzers (NDIR for CO and CO_2), CLD (for NO_x), and possibly for hydrocarbons (instead of FID). Indeed, the use of FTIR at the tailpipe is a commonly accepted technique for research and development (see "Introduction").

Figure 4 gives an overview of the "Results" section summarizing the studies that FTIRs was compared with reference values: (i) calibration gases ("Cylinder"), (ii) reference instrument measuring in parallel with the FTIR at the dilution tunnel or at the tailpipe ("Parallel"), (iii) reference instrument at a different location (FTIR at the tailpipe versus reference at the dilution tunnel) (TP vs. CVS). Only cases where at least two studies were available were taken into account. It should be mentioned that the mean values of slopes or already averaged values do not give the complete scatter of the tests. Furthermore, a different number of tests in each case make any comparisons between different compounds doubtful. On the other hand, it has to be reminded that the results summarize 40 years of experience with a wide range of instruments manufacturers (and users).

The mean differences from the reference values were ±2.5% for CO_2, CO, NO_x, and NH_3, without any particular deviation when FTIR and reference instrument were at different locations. The variability (one standard deviation) of the means was 5% for CO_2 and 10% for the other three gases. Again no particularly higher variability of the "TP vs. CVS" cases. For HCs (THC, NMHC) the mean differences were 5–30% and the variability 30%. Smaller mean differences and variability (10%) was calculated for CH_4. The "TP vs. CVS" cases had similar means and variability. CH_2O had closer to CH_4 behavior, while CH_3CHO was closer to NH_3, but the number of tests was very limited to

draw any conclusions. The results are reasonable, considering that the uncertainty of the different equipment to which FTIR was compared was not the same. As it was discussed in the respective sections, the reference instruments for THCs, NMHCs, and carbonyls have higher uncertainty than those for, e.g., CO_2 and CO. On the one hand, the THC measurement with FID is not specific, as different HCs can have different response factors in the flame; and on the other hand, THC estimate with the FTIR might be not exhaustive, as some HCs can be not quantified if they are not initially included in the calibration method. A proposal to bring closer the two methods was to use a group of HCs as a surrogate to NHMC and then combined it with ethanol, acetaldehyde, and formaldehyde to calculate NMOG [162]. Another way of research may be to apply chemometric tools, such as principal components regression (PCR) and partial least squares regression (PLSR), on the FTIR multivariate data to predict the THC estimated with FID. Either way, a higher uncertainty margin would be necessary when using FTIR to assess compliance to THCs standards.
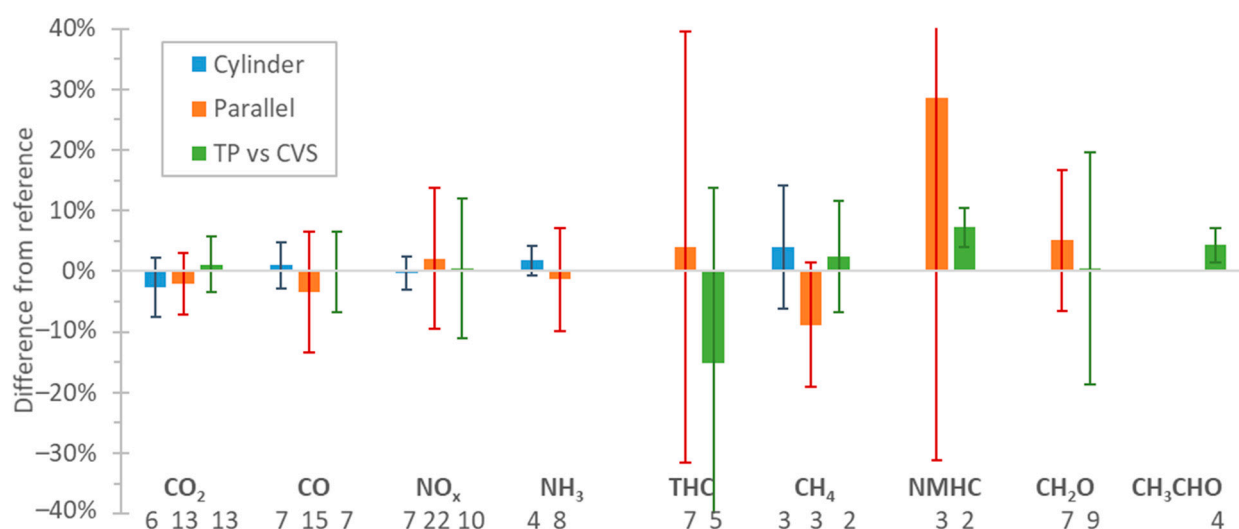
Figure 4. Overview of FTIR assessment studies. For each component, the mean deviations from the reference instruments were calculated based on the studies of Appendix A. "Cylinder" refers to calibration gases. "Parallel" means FTIR and reference instruments were measuring both from the dilution tunnel or the tailpipe. "TP vs. CVS" refers to cases where the FTIR was measuring from the tailpipe, while the reference instrument from the dilution tunnel. Error bars show one standard deviation of at least two studies. Numbers give the number of studies for the calculation of the means.

The analysis was repeated considering only the studies of the last ten years (i.e., 2011 and afterwards), in order to see whether there were any trends of improvements (i.e., closer agreement with the references). For THCs, NMHC, CH_4, and acetaldehyde there were no studies or only one study was available for each case, thus no conclusion could be drawn. For acetaldehyde, practically the same studies remained, thus there was no meaning for any comparison. For CO_2, CO, NO_x, and NH_3, the mean differences and variabilities remained the same or slightly improved (in particular for CO), but without any statistically significant difference (only 2–6 studies available per case).

4.2. FTIR and Interferences

The higher differences for some components when measuring exhaust gas, compared to calibration gases, can be attributed to analytical and sampling interferences. Analytical interference (also called background or spectral interference) occurs when two or more compounds have overlapping absorbance bands in their infrared spectra. To minimize such interferences, appropriate resolution, selection of wave lengths, an appropriate library of expected components, and post-processing of the spectra are necessary [120].

Sampling system interferences are interferences that prohibit or prevent delivery of the target compounds to the FTIR gas cell (e.g., moisture condensation, reactive gases). Regulations, for example, require a heated sampling line (191 °C) when sampling undiluted exhaust in order to avoid the wall adsorption and/or dissolution of hydrophilic compounds (e.g., NH_3, NO_2, aldehydes, or ethanol) in condensed water. A study noticed the delay in oxygenated species reaching the tailpipe during cold start because of their condensation onto cold exhaust system surfaces and dissolution into condensed water [162]. FTIR systems might have differences in real-time operation. It was shown that an FTIR with a slower gas replacement rate and lower sampling frequency was not able to detect some of the rapid concentration fluctuations, e.g., for CO [183]. Another study noticed that during decelerations, the NH_3 concentration did not drop to near zero as it would be expected during fuel cut-offs (NH_3 formation is strongly inhibited by O_2) [184]. Partly the lower response time of the instrument could explain this. However, it was suggested that an important reason was the outgassing of NH_3 from metal surfaces, which act as temporary NH_3 storage reservoirs [184]. A dedicated study on NH_3 found that response attenuation rates were due to mixing and diffusion during transport as well as NH_3 wall storage. Mixing/diffusion effects caused attenuation with a mean time constant of around 1.6 s. Wall storage attenuation had a mean time constant of 72 s [185]. The stored NH_3 on the sampling lines was around 11 mg. It was concluded that, in practical terms, shorter lines at a higher temperature, with flow rates > 10 L/min proved the best for transient response testing [185].

4.3. On-Board Applications

In the previous paragraphs, it was shown that tailpipe application is possible, paying attention to analytical and sampling interferences. Are FTIRs robust enough for on-board applications? Portable systems were already available in the 1980s. However, portable does not necessarily mean suitable for on-board measurements. The main concerns are:

- Size, weight, power consumption.
- Effect of environmental conditions (temperature, altitude, vibrations).
- Safety (liquid N_2 for cooling, other gases on-board, e.g., N_2 for purging).

The importance of size, weight, and power consumption is different for light-duty and heavy-duty applications. The size and weight are very important for light-duty applications, especially for small city cars. Commercial portable FTIRs are split into units that can fit in the vehicle cabin and/or on the hook. The weight without accessories (e.g., pumps, batteries, and heated lines) is around 50 kg, but including accessories is around 100 kg, which is slightly heavier compared to commercial PEMS (portable emissions measurement systems). Even though in the 1980s the need for power generators of 10 kW was reported [186], today's portable systems are <0.5 kW (after warming up in the laboratory). These values are still higher or comparable to PEMS based on other principles. An important point for energy consumption is the location of the sampling pump. If it is located upstream of the FTIR, it needs to be heated, thus the energy consumption will be higher compared to a downstream location. Furthermore, at the downstream location, the pressure can be lower than atmospheric pressure, which is an advantage for on-board measurement because it can be maintained and fixed easier. The liquid N_2 on-board is a concern. One solution is keeping the liquid N_2 in a sealed container, with only one small tube connected, venting the evaporating N_2 to the atmosphere or to the rest of the exhaust gases from the FTIR pump.

The effect of the environmental conditions should be well characterized. FTIRs are sensitive to vibrations: the better the resolution is, the longer the displacement of the moving mirror in the interferometer, and the higher the effect of the vibrations on the optical system. Vibration tests in the late 1990s concluded that FTIRs were best isolated by simply placing them on the rear seat of the vehicle [86]. Today FTIR suppliers claim that their systems are vibrations robust. For example, wire rope isolators can be used [187]. Static single mirror solutions have also been presented [188]. Experiments with NO_x

PEMS (based on CLA or NDUV) showed that sudden temperature changes resulted in zero drift [189]. FTIR results are also sensitive to temperature. The recent CEN standard on PEMS performance prescribes appropriate testing procedures to properly assess the influence of temperature, pressure, and vibrations [190]. Long-term stability and robustness due to vibrations, contamination of optics, etc., should also be assessed.

As with all portable systems, comparison with laboratory versions or other well-established techniques are necessary to increase their confidence in them. Sometimes portable systems might not have the appropriate spectral resolution, response time, or detection limits [104]. For example, in the past, drying of the sample has been used [86], slow response (30 s) [78], or the low optical resolution of $4\,cm^{-1}$ [110] might have negatively affected the accuracy of the results. It should also be emphasized that the studies in Appendix A were with prototype portable systems, thus further studies with commercial systems are needed.

4.4. Regulatory Requirements

It is clear that regulations cannot prescribe in detail all technical aspects of FTIRs. Some basic and important parameters can be described, but appropriate tests are necessary to confirm the instrument's internal hardware and software performances. Table 3 summarizes the technical specifications for FTIRs for NH_3 measurements in the current regulations. Most of them are based on the experience of the users and the capabilities of the instruments. Nevertheless, some specifications could be further restricted or better be controlled for future low emissions vehicles. Such recommendations can be based on recent (2019–2020) standards and methodologies for FTIRs [191–194].

Table 3. Example of technical requirements for FTIR for NH_3 measurements in UNECE Reg. 49.

Specification	Requirement
Sampling line	Stainless steel or PTFE, as short as possible, heated at 190 °C (± 10 °C)
Spectral resolution	$0.5\,cm^{-1}$
Linearity	offset $\leq 0.5\%$ max, slope 0.99–1.01, SEE $\leq 1\%$ max, $R^2 \geq 0.998$
Detection limit	<2 ppm under all conditions of testing
Accuracy	$\pm 3\%$ of the reading or ± 2 ppm, whichever is larger
Zero and span drift	<2% of full scale
Rise time	≤ 5 s
Response time	≤ 20 s

PTFE = polytetrafluoroethylene; SEE = standard error of estimate.

For example, SAE J2992 [192] includes a few more requirements (e.g., repeatability and noise). The detection limit, typically determined with zero gas [191,192], could also be determined using interfering gases [193]. Similarly, in addition to the accuracy test, defined as the deviation of the analyzer reading from the reference value, an interference test could be added. SAE J2992 requires interference testing with a gas containing CO_2, CO, NO_x, and N_2O (mix or separately). For most gases (e.g., NH_3, N_2O, etc.), the maximum total permitted interference is 1%. A spectral residual test is also recommended [191]. USA regulations require appropriate analytical procedures for the interpretation of infrared spectra [193,194].

In the EU RDE regulation, a maximum zero drift of 5 ppm and span drift of 2% is allowed for NO_x. This is much stricter than the 2% of full scale currently prescribed for FTIR. Actually, the drift of FTIR should be negligible as it was discussed before, not only for NH_3, but for all compounds. Thus these drift requirements could be even stricter.

In USA EPA regulations, FTIR analyzer may be used to measure CH_4, C_2H_6, NMHC, and non-methane-non-ethane hydrocarbon (NMNEHC) for continuous sampling for natural gas engines (Title 40/I/U/1065/C/§1065.266). The FTIR analyzer must have combined interferences that are within $\pm 2\%$ (recommended $\pm 1\%$) with CH_4, NMHC, or NMNEHC concentrations expected at the standard (Title 40/I/U/1065/D/§1065.366). Such uncertainties are at the same levels permitted for oxygen interference for FID analyzers.

Furthermore, for regulatory purposes, more quality checks should be included. SAE J2992 has a separate chapter of tests performed prior to and after an emissions cycle test (leak, zero, span, pre- and post-drift checks) [192]. As in CEN/TS 17337, adjustment factors for zero and span, or even zero and span drift could be allowed [191].

4.5. Measurement Uncertainty

One important aspect for future regulations is the uncertainty topic. At the moment, the uncertainty for PEMS analyzers is based on a simple (single point—worst case) model. Assuming a 2 ppm accuracy (including interferences), a 2.5 mg/km uncertainty is calculated for a 3 L engine for the analyzer [107] (see also Table 2). Combining the uncertainty of the exhaust flow, the distance, the trip dynamics, this value could be doubled. This value can be 5 times higher for heavy-duty engines. The values are half of the proposed future NH_3 limits [103]. This means that the accuracy requirement instead of "$\pm3\%$ of the reading or ±2 ppm, whichever is larger", should change, for example, to "$\pm2\%$ of the reading for concentrations > 50 ppm, and ±1 ppm for lower concentrations". This change would significantly reduce the uncertainty if mass limits are set (and not concentration in ppm). CEN/TS 17337, applicable to stationary sources emissions provides a detailed analysis [191]. A big step was the publication of CEN PEMS performance standard, where a second by second calculation is provided for the calculation of the final uncertainty [190]. Related to the uncertainty is also the traceability topic. The regulated gases have reached high levels of accuracy and traceability. However, this is not the case for non-regulated gases. For example, formaldehyde is tricky to calibrate because it tends to polymerize against the cylinder walls of the gas container. An old study found transfer efficiency of formaldehyde of 95.5% ($\pm13.5\%$) for all vehicle types (gasoline, diesel, methanol) [24]. At the time of writing, the uncertainty of the formaldehyde calibration gas is much higher than the 2% uncertainty of the regulated gases. In another study, acetaldehyde standard (25 ppm in N_2) could not be used because an impurity was detected in the gas bottle [168].

5. Conclusions

This review summarized the studies that assessed FTIRs performance on the measurement of vehicle exhaust emissions. The mean differences compared to regulated or other methods were around $\pm2.5\%$ for CO_2, CO, NO_x, and NH_3 with a variability (one standard deviation) of 5% for CO_2 and 10% for CO, NO_x, and NH_3. For CH_4, acetaldehyde, and formaldehyde, the mean differences were $\pm10\%$ (variability 10–20%), but for total hydrocarbons, much higher differences were noticed. The differences were similar regardless of the sampling location of the FTIR (dilution tunnel or tailpipe). Assessment of prototype portable FTIRs on the road confirmed these findings also on-board, but for a narrow range of environmental and driving conditions. Based on these results, FTIRs may be an alternative for on-road testing. However, more studies with commercial portable systems are necessary to cover a wider range of environmental and driving conditions. The introduction of FTIRs in the regulation will require strict technical and performance requirements and procedures based on recently developed standards.

Conflicts of Interest: The authors declare no conflict of interest. The opinions expressed in this manuscript are those of the authors and should in no way be considered to represent an official

opinion of the European Commission. Mention of trade names or commercial products does not constitute endorsement or recommendation by the European Commission or the authors.

Appendix A

The following tables summarize the studies that evaluated FTIRs comparing them with reference values. The following terminology applies:

- Year: Year of the study (published). The studies are given in chronological order; separately for laboratory and portable systems.
- Instrument: Manufacturer and model of the FTIR (as given in the study). In italics in case the FTIR was portable (and the letter "P" is added).
- Difference: Difference of FTIR from the reference value. If many points were available, the mean and the range (in brackets) is given.
- Slope: Linear regression analysis slope.
- R^2: Coefficient of determination of linear regression.
- Range: Concentration or emissions range (from plots or tables of the studies).
- Points: Number of points that the mean or the slope and R2 were calculated.
- Comment: Particularities of the tests and additional information: CNG = compressed natural gas; D = diesel; E = ethanol; FFV = flex-fuel vehicle; G = gasoline; M = methanol; x = number of cars; y = years.
- Ref: Citation of study.

For each study, the following subdivisions were made whenever data were available:

- FTIR measuring cylinder (calibration gas).
- FTIR and reference, both sampling from the dilution tunnel.
- FTIR and reference, both sampling from the tailpipe.
- FTIR sampling from the tailpipe, reference from the dilution tunnel.

Table A1. Comparisons of FTIR with CO_2 analyzers (all NDIR).

Year	Instrument [1]	Difference	Slope	R^2	Range	Points	Comment	Ref.
				FTIR measuring cylinder				
2010	MKS MultiGas 2030	−10.5%	-	-	12%	1	mix with CO, NO, C_3H_8	[95]
2010	AVL Sesam	-	1.01	-	1–14%	10		[195]
2019	AVL Sesam	<1%	-	-	1500 and 15,000 ppm	2		[196]
2005	*P: Temet Gasmet CR2000*	−4.4%	-	-	14.5%	1		[110]
2005	*P: Temet Gasmet CR2000*	−5.4%	-	-	10.0%	1	mix with CO	[110]
2015	*P: Spectrum 2, PerkinElmer*	0.4% (−9%...4%)	1.02	1.00	0–20%	17		[181]
				Both FTIR and reference connected at the dilution tunnel				
1990	Nicolet Sesam	−0.6%	-	-	300–370 g/mi	means	G, Dx2	[165]
1990	Mattson Horiba	-	0.92	0.99	0.4–2.0%	25	G, fuels M85	[112]
1993	Mattson REA	13.7% (0.8%...27%)	1.05	0.98	0.2–1%	380	2.5 y (G, CNG)	[170]
1993	Nicolet REGA	3.0% (−13%...18%)	0.93	0.97	0.2–1%	268	2.5 y (G, CNG)	[170]
1994	Nicolet REGA	−2.8% (−9%...7.5%)	0.96	0.89	0.4–0.6%	12	G	[146]
1994	Nicolet REGA 7000	2.1%	-	-	0.4%	1	G, fuel M85	[171]
				Both FTIR and reference connected at the tailpipe				
1990	Nicolet Sesam	−1.3%	-	-	300–370 g/mi	means	G, Dx2	[165]
2010	AVL Sesam (MKS)	−5%			600–1200 g/kWh	25	G, fuels	[123]
2019	AVL Sesam	±2%	-	-	4–13%	9	G, D, CNG, moped, moto.	[135]
2005	*P: Temet Gasmet CR2000*	3.1%	-	-	12.8%	1	engine	[110]
2005	*P: Temet Gasmet CR2000* [2]	−12.6%	-	-	400 g/km	1	G	[110]
2006	*P: Temet Gasmet CR2000*	-	1.02	0.96	8–15%	cycle	G	[163]
2020	*P: Bruker Matrix MG5* [2]	-	0.99	0.99	<13%	cycle	D	[102]
				FTIR at the tailpipe and reference at the dilution tunnel				
1985	Prototype	-	0.98	0.94	30–340 g/mi	80	G	[164]
1998	VW Sesam	-	1.01	0.96	300–550 g/mi	65	Gx10	[113]
2013	MEXA-6000FT	10% (±1%)	-	-	200 g/km	6	Gx2 (E0–10–20, M15–30)	[179]
2017	Gasmet CR2000		1.06	0.97	140–250 g/km	20	Dx2, Gx2, CNG	[197]
2018	AVL Sesam	±4%	-	-	110–190 g/km	11	D	[61]
2020	AVL Sesam	-	1.01	0.90	200–440 g/km	9	D	[198]
2021	AVL Sesam	0.2% (±0.8%)	-	-	140–650 g/km	37	G	[199]
2006	*P: Temet Gasmet CR2000*	−2.1% (−5%...1%)	-	-	180–230 g/km	11	G	[163]
2018	*P: Nicolet Antaris IGS*	6.4% (−19%...61%)	0.96	0.70	85–300 g/km	18	D, CNG	[98]

[1] *P: portable (in italics)*. [2] Comparison on the road with PEMS.

Table A2. Comparisons of FTIR with CO analyzers (all NDIR).

Year	Instrument [1]	Difference	Slope	R^2	Range	Points	Comment	Ref.
				FTIR measuring cylinder				
2010	MKS MultiGas 2030	−0.8%	-	-	8%	1		[95]
2019	AVL Sesam	<1%	-	-	1000 ppm	4		[196]
2000	*P: Nicolet Protégé 460*	<0.5%	-	-	0–10 ppm	3		[86]
2000	*P: Nicolet*	-	1.02	1.00	0–19 ppm	5–10		[178]
2000	*P: Nicolet*	−3.6%	-	-	19 ppm	2	Mix (CO_2, H_2O)	[178]
2005	*P: Temet Gasmet CR2000*	8.7%	-	-	4900 ppm	1		[110]
2015	*P: Spectrum 2, PerkinElmer*	−1.2% (−30%...15%)	0.99	1.00	0–5000 ppm	15		[181]
			Both FTIR and reference connected at the dilution tunnel					
1990	Nicolet Sesam	−4.2%	-	-	1–10 g/mi	means	G, Dx2	[165]
1990	Mattson Horiba	-	0.80	0.87	0–2500 ppm	25	G, fuels M85	[112]
1991	Bio-Rad Digilab FTS-60	-	0.82	0.96	0–400 ppm	20	Many G, fuels	[169]
1993	Mattson REA	4% (−51%...68%)	0.94	0.98	0–0.8%	390	2.5 y (G, CNG)	[170]
1993	Nicolet REGA	0% (−87%..109%)	1.20	0.86	0–0.8%	268	2.5 y (G, CNG)	[170]
1994	Nicolet REGA	−0.8% (−6%...7%)	0.96	1.00	4–265 ppm	12	G	[146]
1994	Nicolet REGA 7000	0.4%	-	-	178 ppm	1	G, fuel M85	[171]
2000	*P: Nicolet Protégé 460*	3.5%	-	-	5–26 ppm	2	G	[86]
			Both FTIR and reference connected at the tailpipe					
1990	Nicolet Sesam	4.4%	-	-	1–10 g/mi	means	G, Dx2	[165]
2010	AVL Sesam (MKS)	−5%	-	0.99	20–45 g/kWh	25	G, fuels	[123]
2010	AVL Sesam	−2.5% (0% . . . 9%)	-	-	5–170 g/kWh	6	6 snowmobiles	[195]
2005	*P: Temet Gasmet CR2000*	−12%	-	-	2500 ppm	1	engine	[110]
2005	*P: Temet Gasmet CR2000* [2]	1.3%	-	-	10 g/km	1	G	[110]
2006	*P: Temet Gasmet CR2000*	-	0.87	0.99	0–6000 ppm	cycle	G	[163]
2020	*P: Bruker Matrix MG5* [2]	-	1.00	0.98	0–2000 ppm	cycle	D	[102]
			FTIR at the tailpipe and reference at the dilution tunnel					
1985	Prototype	-	1.04	0.98	0–37 g/mi	80	G	[164]
1998	VW Sesam	-	1.08	0.99	0–6 g/mi	65	Gx10	[113]
2013	MEXA-6000FT	5.8% (−4%...8%)	-	-	0.27–0.37 g/km	6	Gx2 (E0–10–20, M15–30)	[179]
2017	Gasmet CR2000		0.95	0.97	50–3000 mg/km	15	Dx2, Gx2, CNG	[197]
2006	*P: Temet Gasmet CR2000*	−1.5% (−11%.4%)	0.95	0.98	0.5–1.1 g/km	11	G	[163]
2007	*P: Nicolet*	-	0.90	0.90	0.1–1.1 g/mi	15	Gx4	[92]
2018	*P: Nicolet Antaris IGS*	−4.7% (−75%...69%)	1.01	0.92	10–400 mg/km	18	D, CNG	[98]

[1] *P: portable (in italics)*. [2] Comparison on the road with PEMS.

Table A3. Comparisons of FTIR with NO_x analyzers (all CLD unless otherwise specified).

Year	Instrument [1]	Difference	Slope	R^2	Range	Points	Comment	Ref.
				FTIR measuring cylinder				
2010	MKS MultiGas 2030	3.5%	-	-	4000 ppm	1		[95]
2010	AVL Sesam	-	1.00	-	0–4000 ppm	14		[195]
2000	P: Nicolet	-	0.95	1.00	0–3 ppm	5–10		[178]
2000	P: Nicolet	−2.1% and 1.1%	-	-	3 ppm	2	Mix (CO_2, H_2O)	[178]
2000	P: Nicolet Protégé 460	±10%	-	-	1–10 ppm	5		[86]
2005	P: Temet Gasmet CR2000	0.3%	-	-	1451 ppm	1		[110]
			Both FTIR and reference connected at the dilution tunnel					
1990	Nicolet Sesam	−5.2%	-	-	0.5–1 g/mi	means	G, Dx2	[165]
1990	Mattson Horiba	-	0.95	0.94	0–50 ppm	25	G, fuels M85	[112]
1991	Bio-Rad Digilab FTS-60	-	0.93	0.89	0–40 ppm	20	Many G, fuels	[169]
1993	Mattson REA	4% (−40%...48%)	1.04	0.78	0–100 ppm	368	2.5 y (G, CNG)	[170]
1993	Nicolet REGA	32% (−31%..86%)	1.36	0.97	0–100 ppm	217	2.5 y (G, CNG)	[170]
1994	Nicolet REGA	−6.6% (−11%.1%)	0.96	1.00	4–14 ppm	12	G	[146]
1994	Nicolet REGA 7000	1.0%	-	-	3 ppm	1	G, fuel M85	[171]
2015	AVL Sesam	1.3%...10.5%	-	-	40–80 ppm	2	Dx2	[140]
2000	P: Nicolet Protégé 460	0.5%	-	-	0.5–3 ppm	2	G	[86]
			Both FTIR and reference connected at the tailpipe					
1990	Nicolet Sesam	8.0%	-	-	0.5–1 g/mi	means	G, Dx2	[165]
1996	Nicolet REGA 7000	−10%	-	-	0–4000 ppm	cycle	G	[30]
2010	AVL Sesam (MKS)	5%	-	1.00	8–20 g/kWh	25	G, fuels	[123]
2010	Nicolet Magna 560	5.4% (3%..9%)	-	-	20–100 ppm	4	CNG + NO_2 injection	[142]
2016	Not disclosed	<5%	-	-	300–1000 ppm	steady	D	[200]
2018	AVL Sesam (MKS)	-	1.03	1.00	0–600 ppm	600	various	[141]
2018	AVL Sesam	4% (±9%)	-	-	50–1200 mg/km	22	D	[61]
2000	P: Nicolet	± 5%	-	-	0–70 ppm	cycle	G	[178]
2005	P: Temet Gasmet CR2000	13%	-	-	70 ppm	1	engine	[110]
2005	P: Temet Gasmet CR2000 [2]	−30%	-	-	1.9 g/km	1	G	[110]
2006	P: Temet Gasmet CR2000	-	1.05	0.94	0–800 ppm	cycle	G	[163]
2017	P: MIDAC I-series [2]	-	1.09	0.99	0–400 ppm	cycle	D	[201]
2020	P: Bruker Matrix MG5 [2]	-	1.03	0.97	0–1000 ppm	cycle	D	[102]
			FTIR at the tailpipe and reference at the dilution tunnel					
1985	Prototype	-	0.98	0.97	0–3.2 g/mi	80	G	[164]
1998	VW Sesam	-	0.98	0.99	0–0.8 g/mi	65	Gx10	[113]
2013	MEXA-6000FT	7.1% (5%...10%)	-	-	0.5 g/km	6	Gx2 (E0–10–20, M15–30)	[179]

Table A3. *Cont.*

Year	Instrument [1]	Difference	Slope	R^2	Range	Points	Comment	Ref.
2015	AVL Sesam	−8.8%...3.0%	-	-	190–310 ppm	4	D	[140]
2018	AVL Sesam	11% (±10%)	-	-	50–1200 mg/km	22	D	[61]
2020	AVL Sesam	-	0.94	0.79	0–350 mg/km	9	D	[198]
2017	Gasmet CR2000	-	0.79	0.99	10–1200 mg/km	12	Dx2, Gx2, CNG	[197]
2006	*P: Temet Gasmet CR2000*	3.6% (2.7%...4%)	-	-	0.2–0.3 g/km	11	G	[163]
2007	*P: Nicolet*	-	1.02	0.96	5–40 mg/mi	8	Gx4	[92]
2018	*P: Nicolet Antaris IGS*	32% (−22%...117%)	1.21	0.92	5–650 mg/km	18	D, CNG	[98]

[1] *P: portable (in italics).* [2] Comparison on the road with PEMS.

Table A4. Comparisons of FTIR with NH_3 analyzers (FTIR, QCL, LDS).

Year	Instrument [1]	Difference	Slope	R^2	Range	Points	Comment	Ref.
			FTIR measuring cylinder					
2009	AVL Sesam	± 5%	-	-	20 ppm	1	Daily checks	[202]
2012	AVL Sesam	−0.2%	-	-	100 ppm	1		[203]
2016	Horiba	<2.5%	-	-	100 ppm	1		[150]
2016	Not disclosed	<5%	-	-	0–350 ppm	3	D engine NH_3 injection	[200]
			Both FTIRs connected at the tailpipe					
2016	Horiba	<2.5%	-	-	50 ppm	1	D	[150]
2017	*P: MIDAC I-series*	-	1.03	0.80	0–300 ppm	cycle	G	[201]
2020	*P: Bruker Matrix MG5*	-	0.82	0.96	0–100 ppm	cycle	D	[102]
			Both FTIR and QCL connected at the tailpipe					
2011	Horiba	0–5%	-	-	0–350 ppm	many	D and NH_3 injection	[147]
2015	MKS 2030-HS	−6%	1.09	1.00	0–25 ppm	4	Dx2, G, FFV	[151]
2020	Not disclosed	-	0.98	0.99	25–100 ppm	cycle	D	[204]
			Both FTIR and LDS or CI-MS at the tailpipe					
2018	Gasmet DX4000 [2]	−9% (−19%...1%)	-	-	0–25 ppm	5	D	[149]
2004	Nicolet Avatar 370 [3]	-	1.01	0.99	25–100 ppm	cycle	G	[152]

[1] *P: portable (in italics).* [2] vs. LDS. [3] vs. CI-MS.

Table A5. Comparisons of FTIR with THC analyzers (FID).

Year	Instrument [1]	Difference	Slope	R^2	Range	Points	Comment	Ref.
			Both FTIRs connected at the dilution tunnel					
1985	Prototype	-	1.34	0.97	0–3.7 g/mi	80	G	[164]
1990	Nicolet Sesam	1.9% (−2%...1%)	-	-	0.2–0.9 g/mi	means	G, Dx2	[165]
1990	Mattson Horiba	-	1.13	0.99	0–1200 ppm	25	G (fuels, M85)	[112]
			Both FTIR and reference (FID) connected at the tailpipe					
1990	Nicolet Sesam	17.6% (1%...38%)	-	-	0.2–0.9 g/mi	means	G, Dx2	[165]
1996	Nicolet REGA 7000	−15%	-	-	<10,000 ppm	cycles	G	[30]
2005	*P: Temet Gasmet CR2000*	−66%, −63%	-	-	600 ppm		engine G, G	[110]
2006	*P: Temet Gasmet CR2000*	−55%	0.41	0.99	0–1600 ppm	cycle	G	[163]
			FTIR at the tailpipe and reference at the dilution tunnel					
1994	Nicolet REGA 7000	1.8% (−4%...4%)	-	-	50 ppm	5	CNG	[171]
1998	VW Sesam		1.09	0.97	<0.4 g/mi	65	Gx10	[113]
2000	*P: Nicolet*	5%	-	-	550 mg/mi	1	G	[178]
2006	*P: Temet Gasmet CR2000*	−55% (−5% cal.)	-	-	160 mg/km	10	G	[163]
2018	*P: Nicolet Antaris IGS*	46% (−63%...280%)	0.63	0.69	0–300 mg/km	16	D, CNG	[98]

[1] *P: portable (in italics).*

Table A6. Comparisons of FTIR with CH_4 analyzers (FID), unless specified otherwise.

Year	Instrument [1]	Difference	Slope	R^2	Range	Points	Comment	Ref.
				FTIR measuring cylinder				
1992	Nicolet REGA 7000	15%	-	-	15–17 ppm	2	Mix	[166]
2005	*P: Temet Gasmet CR2000*	−5.1%	-	-	1509 ppm	1		[110]
2015	*P: Spectrum 2, Perkin Elmer*	1.0% (−2.4%...7.1%)	1.02	1.00	0–50%	17		[181]
		Both FTIRs connected at the dilution tunnel (or tailpipe if specified)						
1991	Bio-Rad Digilab FTS-60	-	0.89	0.96	0–10 ppm	20	Many G, fuels	[169]
1994	Nicolet REGA 7000	−17.9%	-	-	3 ppm	1	G (M85)	[171]
2016	Thermo Fisher Antaris IGS	2.4% (0.8%...4.2%)	-	-	1500–3000 ppm	12	D-CNG	[167]
		FTIR at the tailpipe and reference at the dilution tunnel						
1998	VW Sesam	-	1.09	0.99	0–0.07 g/mi	65	Gx10	[113]
2020	AVL Sesam	-	0.96	0.99	0–40 mg/km	9	D	[198]
		FTIR versus FTIR or GS						
1994	Nicolet REGA 7000 [2]	5%	-	-	43 ppm	1	CNG	[171]
1994	Sesam II [3]	5% (−29%...20%)	1.11	0.99	40–250 ppm	12	G	[180]
2017	Gasmet CR2000 [2]	-	0.97	0.95	3–105 mg/km	17	Dx2, Gx2, CNG	[197]
2020	*P: Bruker Matrix MG5* [3]	-	1.07	0.93	0–6000 ppm	cycle	D	[102]

[1] *P: portable (in italics).* [2] vs. GS. [3] vs. FTIR

Table A7. Comparisons of FTIR with NMHC analyzers (FID).

Year	Instrument [1]	Difference	Slope	R^2	Range	Points	Comment	Ref.
				FTIRs measuring cylinder				
2000	*P: Nicolet Protégé 460*	0–9%	-	-	1–10 ppm	3		[86]
		Both FTIRs connected at the dilution tunnel (or tailpipe if specified)						
1991	Bio-Rad Digilab FTS-60	-	1.03	0.96	0–120 ppm	20	Many G, fuels	[169]
2000	*P: Nicolet Protégé 460*	−14%...−5%	-	-	2 and 8 ppm	2	G	[86]
2016	Thermo Fisher Antaris IGS	97% (31%...292%)	-	-	50–350 ppm	12	D-CNG	[167]
		FTIR at the tailpipe and reference at the dilution tunnel						
2007	*P: Nicolet*	9.5% (−32%...52%)	1.04	0.99	3–51 mg/mi	8	Gx4	[92]
2017	AVL Sesam	5%	0.95–1.05	-	0–2500 ppm	many	G, FFV (E10, E50, E85)	[162]

[1] *P: portable (in italics).*

Table A8. Comparisons of FTIR with formaldehyde (CH_2O) methodology (DNPH + HPLC).

Year	Instrument [1]	Difference	Slope	R^2	Range	Points	Comment	Ref.
		FTIR connected at the dilution tunnel						
1986	Prototype	-	1.01	0.99	0.3–8.5 ppm	78	G (methanol)	[24]
1990	Mattson Horiba	-	1.03	0.99	0–80 ppm	25	G, fuels M85	[112]
1992	Nicolet REGA 7000	17%	1.14	0.99	0–45 mg/mi	6	G	[166]
1993	Mattson REA	18% (−60%...98%)	1.25	0.91	0–4 ppm	206	2.5 y (G, CNG)	[170]
1993	Nicolet REGA	34% (−33%...96%)	1.04	0.95	0–4 ppm	229	2.5 y (G, CNG)	[170]
1994	Nicolet REGA 7000	0.9%	-	-	10 ppm	1	G, fuel M85	[171]
1994	Sesam II	−13% (−21%...−6%)	0.88	0.88	2–16 ppm	6	G	[180]
		FTIR at the tailpipe and reference at the dilution tunnel						
1990	Nicolet Sesam	-	0.85	0.94	3–72 mg/mi	15	G, Dx2	[165]
1991	Bio-Rad Digilab FTS-60	-	0.84	0.97	0–8 ppm	20	Many G, fuels	[169]
1998	VW Sesam	-	0.68	0.57	0–4 mg/mi	65	Gx10	[113]
1998	VW Sesam	15%	-	-	2 mg/mi	2	G	[113]
2006	MEXA 4000 FT	-	1.01	0.91	0–6 ppm	26	D	[176]
2013	MEXA 6000 FT	−0.5% (−2.2%...2.4%)	-	-	2 mg/km (<60 ppm)	6	Gx2 (E0–10–20, M15–30)	[179]
2016	AVL Sesam	−5%...27%	-	-	0–4 mg/km	3	Motorcycle (flexi)	[205]
2017	Gasmet CR2000	-	1.32	0.98	0–20 mg/km	20	Dx2, Gx2, CNG	[197]
2017	MKS, Sesam, MEXA	8% (−4%...32%)	-	0.82–0.94	0–8 mg/km	8	FFV	[168]

Table A9. Comparisons of FTIR with acetaldehyde (CH_3CHO) methodology (DNPH + HPLC).

Year	Instrument [1]	Difference	Slope	R^2	Range	Points	Comment	Ref.
		FTIR connected at the dilution tunnel						
2010	Gasmet CR2000	−20%, +5%	-	-	10–35 mg/km	2	FFV (E5, E85)	[160]
		FTIR at the tailpipe and reference at the dilution tunnel						
2006	MEXA 4000 FT	-	2.45	0.79	0–2 ppm	27	D	[176]
2013	MEXA 6000 FT	2.2% (−1%...5%)	-	-	1–2 mg/km (<100 ppm)	3	Gx2 (E0, E10, E20)	[179]
2016	AVL Sesam	−1%...5%	-	-	0–35 mg/km	3	Motorcycle (flex-fuel)	[205]
2017	Gasmet CR2000	-	1.08	0.90	0–27 mg/km	22	Dx2, Gx2, CNG	[197]
2017	MKS, Sesam, MEXA	5% (0%...9%)	-	-	0–43 mg/km	8	FFV	[168]

References

1. Berg, W. Legislation for the reduction of exhaust gas emissions. In *Traffic and Environment*; Gruden, D., Ed.; Springer: Berlin/Heidelberg, Germany, 2003; Volume 3T, pp. 175–253. ISBN 978-3-540-00050-1.
2. Keenan, M. *Exhaust Emissions Control: 60 Years of Innovation and Development*; SAE Technical Paper 2017-24-0120: Warrendale, PA, USA, 2017. [CrossRef]
3. Smith, B.C. *Fundamentals of Fourier Transform Infrared Spectroscopy*, 2nd ed.; CRC Press: Boca Raton, FL, USA, 2011; ISBN 978-1-4200-6929-7.
4. Guerrero-Pérez, M.O.; Patience, G.S. Experimental Methods in Chemical Engineering: Fourier Transform Infrared Spectroscopy—FTIR. *Can. J. Chem. Eng.* **2020**, *98*, 25–33. [CrossRef]
5. Doyle, G.J.; Tuazon, E.C.; Graham, R.A.; Mischke, T.M.; Winer, A.M.; Pitts, J.N. Simultaneous Concentrations of Ammonia and Nitric Acid in a Polluted Atmosphere and Their Equilibrium Relationship to Particulate Ammonium Nitrate. *Environ. Sci. Technol.* **1979**, *13*, 1416–1419. [CrossRef]
6. Tuazon, E.C.; Winer, A.M.; Pitts, J.N. Trace Pollutant Concentrations in a Multiday Smog Episode in the California South Coast Air Basin by Long Path Length Fourier Transform Infrared Spectroscopy. *Environ. Sci. Technol.* **1981**, *15*, 1232–1237. [CrossRef] [PubMed]
7. Herget, W.F.; Brasher, J.D. Remote Measurement of Gaseous Pollutant Concentrations Using a Mobile Fourier Transform Interferometer System. *Appl. Opt.* **1979**, *18*, 3404–3420. [CrossRef]
8. Herget, W.F.; Lowry, S.R. Auto Exhaust Gas Analysis by FTIR Spectroscopy. In Proceedings of the Optics, Electro-Optics, and Laser Applications in Science and Engineering, Los Angeles, CA, USA, 20–25 January 1991; Proc. SPIE 1433 Measurement of Atmospheric Gases; pp. 275–289. [CrossRef]
9. Allen, D.T.; Palen, E. Recent Advances in Aerosol Analysis by Infrared Spectroscopy. *J. Aerosol Sci.* **1989**, *20*, 441–455. [CrossRef]
10. Takahama, S.; Dillner, A.M.; Weakley, A.T.; Reggente, M.; Bürki, C.; Lbadaoui-Darvas, M.; Debus, B.; Kuzmiakova, A.; Wexler, A.S. Atmospheric Particulate Matter Characterization by Fourier Transform Infrared Spectroscopy: A Review of Statistical Calibration Strategies for Carbonaceous Aerosol Quantification in US Measurement Networks. *Atmos. Meas. Tech.* **2019**, *12*, 525–567. [CrossRef]
11. Lu, P.-D.; He, T.; Zhang, Y.-H. Relative Humidity Anneal Effect on Hygroscopicity of Aerosol Particles Studied by Rapid-Scan FTIR-ATR Spectroscopy. *Geophys. Res. Lett.* **2008**, *35*. [CrossRef]
12. Liu, J.; Wang, L.; Sun, P.; Wang, P.; Li, Y.; Ma, H.; Wu, P.; Liu, Z. Effects of Iron-Based Fuel Borne Catalyst Addition on Microstructure, Element Composition and Oxidation Activity of Diesel Exhaust Particles. *Fuel* **2020**, *270*, 117597. [CrossRef]
13. Mao, Z.; Demirgian, J.; Mathew, A.; Hyre, R. Use of Fourier Transform Infrared Spectrometry as a Continuous Emission Monitor. *Waste Manag.* **1995**, *15*, 567–577. [CrossRef]
14. Bradley, K.S.; Brooks, K.B.; Hubbard, L.K.; Popp, P.J.; Stedman, D.H. Motor Vehicle Fleet Emissions by OP-FTIR. *Environ. Sci. Technol.* **2000**, *34*, 897–899. [CrossRef]
15. Phillips, F.A.; Naylor, T.; Forehead, H.; Griffith, D.W.T.; Kirkwood, J.; Paton-Walsh, C. Vehicle Ammonia Emissions Measured in an Urban Environment in Sydney, Australia, Using Open Path Fourier Transform Infra-Red Spectroscopy. *Atmosphere* **2019**, *10*, 208. [CrossRef]
16. Schäfer, K.; Heland, J.; Lister, D.H.; Wilson, C.W.; Howes, R.J.; Falk, R.S.; Lindermeir, E.; Birk, M.; Wagner, G.; Haschberger, P.; et al. Nonintrusive Optical Measurements of Aircraft Engine Exhaust Emissions and Comparison with Standard Intrusive Techniques. *Appl. Opt.* **2000**, *39*, 441–455. [CrossRef] [PubMed]
17. Vojtisek-Lom, M.; Jirků, J.; Pechout, M. Real-World Exhaust Emissions of Diesel Locomotives and Motorized Railcars during Scheduled Passenger Train Runs on Czech Railroads. *Atmosphere* **2020**, *11*, 582. [CrossRef]
18. Lechner, B.; Paar, H.; Sturm, P.J. Measurement of VOCs in Vehicle Exhaust by Extractive FTIR Spectroscopy. In Proceedings of the Europto Remote Sensing, SPIE, Barcelona, Spain, 25–29 September 2000; Fujisada, H., Lurie, J.B., Ropertz, A., Weber, K., Eds.; Proc. SPIE 4169; pp. 432–439. [CrossRef]
19. Bacsik, Z.; Mink, J.; Keresztury, G. FTIR Spectroscopy of the Atmosphere Part 2. Applications. *Appl. Spectrosc. Rev.* **2005**, *40*, 327–390. [CrossRef]
20. Simonescu, M.C. Application of FTIR spectroscopy in environmental studies. In *Advanced Aspects of Spectroscopy*; Farrukh, M.A., Ed.; InTech: London, UK, 2012; ISBN 978-953-51-0715-6.
21. Butler, J.W.; Maker, P.D.; Korniski, T.J.; Haack, L.P. *On-Line Characterization of Vehicle Emissions by FT-IR and Mass Spectrometry*; SAE Technical Paper 810429: Warrendale, PA, USA, 1981. [CrossRef]
22. Staab, J.; Klingenberg, H.; Schürmann, D. *Strategy for the Development of a New Multicomponent Exhaust Emissions Measurement Technique*; SAE Technical Paper 830437: Warrendale, PA, USA, 1983. [CrossRef]
23. Staab, J.; Klingenberg, H.; Pflüger, H.; Herget, W.F.; Tromp, M.I. *First Experiences in Testing a New Multicomponent Exhaust Gas Sampling and Analyzing System*; SAE Technical Paper 851659: Warrendale, PA, USA, 1985. [CrossRef]
24. Haack, L.P.; LaCourse, D.L.; Korniski, T.J. Comparison of Fourier Transform Infrared Spectrometry and 2,4-Dinitrophenylhydrazine-Impinger Techniques for the Measurement of Formaldehyde in Vehicle Exhaust. *Anal. Chem.* **1986**, *58*, 68–72. [CrossRef]

25. Adachi, M.; Yamagishi, Y.; Inoue, K.; Ishida, K. *Automotive Emission Analyses Using FTIR Spectrophotometer*; SAE Technical Paper 920723: Warrendale, PA, USA, 1992. [CrossRef]

26. Zweidinger, R.A.; Crews, W.S.; Braddock, J.N. *Comparison of Three Analytical Methods for the Determination of Methanol in Vehicle Evaporative and Exhaust Samples*; SAE Technical Paper 930377: Warrendale, PA, USA, 1993. [CrossRef]

27. Laurikko, J.; Aakko, P. *The Effect of Ambient Temperature on the Emissions of Some Nitrogen Compounds:A Comparative Study on Low-, Medium- and High-Mileage Three-Way Catalyst Vehicles*; SAE Technical Paper 950933: Warrendale, PA, USA, 1995. [CrossRef]

28. Bianchi, D.; Gass, J.L.; Bouly, C.; Maret, D. *Determination of Efficiency of Exhaust Gas Catalyst by FTIR Spectroscopy*; SAE Technical Paper 910839: Warrendale, PA, USA, 1991. [CrossRef]

29. Laurikko, J.; Nylund, N.-O. *Regulated and Unregulated Emissions from Catalyst Vehicles at Low Ambient Temperatures*; SAE Technical Paper 930946: Warrendale, PA, USA, 1993. [CrossRef]

30. Lee, G.R.; McDonald, C.R.; Widdicombe, K.A.; van den Brink, P.J. *The Role of Methane on Catalyst Conversion of NOx: Study Based on FTIR*; SAE Technical Paper 961155: Warrendale, PA, USA, 1996. [CrossRef]

31. Adachi, M. Emission Measurement Techniques for Advanced Powertrains. *Meas. Sci. Technol.* **2000**, *11*, R113–R129. [CrossRef]

32. Babu, P.R.; Nagalingam, B.; Mehta, P.S. *Hydrocarbon Modeling for Two-Stroke SI Engine*; SAE Technical Paper 940403: Warrendale, PA, USA, 1994. [CrossRef]

33. Ambs, J.L.; McClure, B.T. *The Influence of Oxidation Catalysts on NO_2 in Diesel Exhaust*; SAE Technical Paper 932494: Warrendale, PA, USA, 1993. [CrossRef]

34. Arai, M. Continuous Analysis of Vehicle Exhaust Gas by Fourier-Transform Infrared Spectroscopy. *Anal. Sci.* **1993**, *9*, 77–82. [CrossRef]

35. Soltani, S.; Andersson, R.; Andersson, B. The Effect of Exhaust Gas Composition on the Kinetics of Soot Oxidation and Diesel Particulate Filter Regeneration. *Fuel* **2018**, *220*, 453–463. [CrossRef]

36. Stanciulescu, M.; Charland, J.-P.; Kelly, J.F. Effect of Primary Amine Hydrocarbon Chain Length for the Selective Catalytic Reduction of NOx from Diesel Engine Exhaust. *Fuel* **2010**, *89*, 2292–2298. [CrossRef]

37. Zhao, W.; Liu, Y.; Wei, H.; Zhang, R.; Luo, G.; Hou, H.; Chen, S.; Zhang, R. NO Removal by Plasma-Enhanced NH3-SCR Using Methane as an Assistant Reduction Agent at Low Temperature. *Appl. Sci.* **2019**, *9*, 2751. [CrossRef]

38. Davies, C.; Thompson, K.; Cooper, A.; Golunski, S.; Taylor, S.H.; Bogarra Macias, M.; Doustdar, O.; Tsolakis, A. Simultaneous Removal of NOx and Soot Particulate from Diesel Exhaust by In-Situ Catalytic Generation and Utilisation of N_2O. *Appl. Catal. B Environ.* **2018**, *239*, 10–15. [CrossRef]

39. Wang, C.; Zhang, C.; Zhao, Y.; Yan, X.; Cao, P. Poisoning Effect of SO_2 on Honeycomb Cordierite-Based Mn–Ce/Al_2O_3 Catalysts for NO Reduction with NH3 at Low Temperature. *Appl. Sci.* **2018**, *8*, 95. [CrossRef]

40. Auvinen, P.; Nevalainen, P.; Suvanto, M.; Oliva, F.; Llamas, X.; Barciela, B.; Sippula, O.; Kinnunen, N.M. A Detailed Study on Regeneration of SO_2 Poisoned Exhaust Gas after-Treatment Catalysts: In Pursuance of High Durability and Low Methane, NH_3 and N_2O Emissions of Heavy-Duty Vehicles. *Fuel* **2021**, *291*, 120223. [CrossRef]

41. de Melo, T.C.C.; Machado, G.B.; Belchior, C.R.; Colaço, M.J.; Barros, J.E.; de Oliveira, E.J.; de Oliveira, D.G. Hydrous Ethanol–Gasoline Blends—Combustion and Emission Investigations on a Flex-Fuel Engine. *Fuel* **2012**, *97*, 796–804. [CrossRef]

42. Gailis, M.; Pirs, V.; Jansons, M.; Birzietis, G.; Dukulis, I. *An Experimental Investigation on Aldehyde and Methane Emissions from Hydrous Ethanol and Gasoline Fueled SI Engine*; SAE Technical Paper 2020-01-2047: Warrendale, PA, USA, 2020. [CrossRef]

43. Liu, S.; Chen, W.; Zhu, Z.; Jiang, S.; Ren, T.; Guo, H. A Review of the Developed New Model Biodiesels and Their Effects on Engine Combustion and Emissions. *Appl. Sci.* **2018**, *8*, 2303. [CrossRef]

44. Tan, P.; Hu, Z.; Lou, D.; Li, Z. Exhaust Emissions from a Light-Duty Diesel Engine with Jatropha Biodiesel Fuel. *Energy* **2012**, *39*, 356–362. [CrossRef]

45. Yu-sheng, Z.; Chun-lan, M.; Hai-ying, S.; Shao-ren, Z. *Study on Formaldehyde Emission in a DME-Fueled Direct-Injection Diesel Engine*; SAE Technical Paper 2007-01-1909: Warrendale, PA, USA, 2007. [CrossRef]

46. Hunicz, J.; Matijošius, J.; Rimkus, A.; Kilikevičius, A.; Kordos, P.; Mikulski, M. Efficient Hydrotreated Vegetable Oil Combustion under Partially Premixed Conditions with Heavy Exhaust Gas Recirculation. *Fuel* **2020**, *268*, 117350. [CrossRef]

47. Lemel, M.; Hultqvist, A.; Vressner, A.; Nordgren, H.; Persson, H.; Johansson, B. *Quantification of the Formaldehyde Emissions from Different HCCI Engines Running on a Range of Fuels*; SAE Technical Paper 2005-01-3724: Warrendale, PA, USA, 2005. [CrossRef]

48. Jiang, C.; Huang, G.; Liu, G.; Qian, Y.; Lu, X. Optimizing Gasoline Compression Ignition Engine Performance and Emissions: Combined Effects of Exhaust Gas Recirculation and Fuel Octane Number. *Appl. Therm. Eng.* **2019**, *153*, 669–677. [CrossRef]

49. Wu, Y.; Wang, P.; Farhan, S.M.; Yi, J.; Lei, L. Effect of Post-Injection on Combustion and Exhaust Emissions in DI Diesel Engine. *Fuel* **2019**, *258*, 116131. [CrossRef]

50. Brosha, E.L.; Prikhodko, V.Y.; Kreller, C.R.; Pihl, J.A.; Curran, S.; Parks, J.E.; Mukundan, R. Response Characteristics of Stable Mixed-Potential NH_3 Sensors in Diesel Engine Exhaust. *Emiss. Control Sci. Technol.* **2017**, *3*, 112–121. [CrossRef]

51. Zarante, P.H.B.; Sodré, J.R. Comparison of Aldehyde Emissions Simulation with FTIR Measurements in the Exhaust of a Spark Ignition Engine Fueled by Ethanol. *Heat Mass Transf.* **2018**, *54*, 2079–2087. [CrossRef]

52. Zardini, A.A.; Suarez-Bertoa, R.; Forni, F.; Montigny, F.; Otura-Garcia, M.; Carriero, M.; Astorga, C. Reducing the Exhaust Emissions of Unregulated Pollutants from Small Gasoline Engines with Alkylate Fuel and Low-Ash Lube Oil. *Environ. Res.* **2019**, *170*, 203–214. [CrossRef]

53. Yamada, H.; Misawa, K.; Suzuki, D.; Tanaka, K.; Matsumoto, J.; Fujii, M.; Tanaka, K. Detailed Analysis of Diesel Vehicle Exhaust Emissions: Nitrogen Oxides, Hydrocarbons and Particulate Size Distributions. *Proc. Combust. Inst.* **2011**, *33*, 2895–2902. [CrossRef]

54. Clairotte, M.; Suarez-Bertoa, R.; Zardini, A.A.; Giechaskiel, B.; Pavlovic, J.; Valverde, V.; Ciuffo, B.; Astorga, C. Exhaust Emission Factors of Greenhouse Gases (GHGs) from European Road Vehicles. *Environ. Sci. Eur.* **2020**, *32*, 125. [CrossRef]

55. Nevius, T.; Rooney, R.; Zummer, R. *Speciation of Nitrogen Oxides in a Light Duty Diesel Engine during an EGR System Failure*; SAE Technical Paper 2012-01-0876: Warrendale, PA, USA, 2012. [CrossRef]

56. Aakko-Saksa, P.; Koponen, P.; Roslund, P.; Laurikko, J.; Nylund, N.-O.; Karjalainen, P.; Rönkkö, T.; Timonen, H. Comprehensive Emission Characterisation of Exhaust from Alternative Fuelled Cars. *Atmos. Environ.* **2020**, *236*, 117643. [CrossRef]

57. Suarez-Bertoa, R.; Kousoulidou, M.; Clairotte, M.; Giechaskiel, B.; Nuottimäki, J.; Sarjovaara, T.; Lonza, L. Impact of HVO Blends on Modern Diesel Passenger Cars Emissions during Real World Operation. *Fuel* **2019**, *235*, 1427–1435. [CrossRef]

58. Bielaczyc, P.; Szczotka, A.; Woodburn, J. An Overview of Emissions of Reactive Nitrogen Compounds from Modern Light Duty Vehicles Featuring SI Engines. *Combust. Engines* **2014**, *159*, 48–53. [CrossRef]

59. Andersson, J.; May, J.; Favre, C.; Bosteels, D.; de Vries, S.; Heaney, M.; Keenan, M.; Mansell, J. On-Road and Chassis Dynamometer Evaluations of Emissions from Two Euro 6 Diesel Vehicles. *SAE Int. J. Fuels Lubr.* **2014**, *7*, 919–934. [CrossRef]

60. Suarez-Bertoa, R.; Astorga, C. Impact of Cold Temperature on Euro 6 Passenger Car Emissions. *Environ. Pollut.* **2018**, *234*, 318–329. [CrossRef] [PubMed]

61. Giechaskiel, B.; Suarez-Bertoa, R.; Lähde, T.; Clairotte, M.; Carriero, M.; Bonnel, P.; Maggiore, M. Evaluation of NOx Emissions of a Retrofitted Euro 5 Passenger Car for the Horizon Prize "Engine Retrofit". *Environ. Res.* **2018**, *166*, 298–309. [CrossRef]

62. Giechaskiel, B.; Suarez-Bertoa, R.; Lahde, T.; Clairotte, M.; Carriero, M.; Bonnel, P.; Maggiore, M. Emissions of a Euro 6b Diesel Passenger Car Retrofitted with a Solid Ammonia Reduction System. *Atmosphere* **2019**, *10*, 180. [CrossRef]

63. Hirschberger, R. Automotive Emissions Analysis with Spectroscopic Techniques. In *Encyclopedia of Analytical Chemistry: Applications, Theory and Instrumentation*, 1st ed.; Meyers, R., Ed.; Wiley: New York, NY, USA, 2006; ISBN 978-0-471-97670-7.

64. Aakko-Saksa, P.; Rantanen-Kolehmainen, L.; Koponen, P.; Engman, A.; Kihlman, J. Biogasoline Options—Possibilities for Achieving High Bio-Share and Compatibility with Conventional Cars. *SAE Int. J. Fuels Lubr.* **2011**, *4*, 298–317. [CrossRef]

65. Aakko-Saksa, P.T.; Rantanen-Kolehmainen, L.; Skyttä, E. Ethanol, Isobutanol, and Biohydrocarbons as Gasoline Components in Relation to Gaseous Emissions and Particulate Matter. *Environ. Sci. Technol.* **2014**, *48*, 10489–10496. [CrossRef]

66. Suarez-Bertoa, R.; Zardini, A.A.; Keuken, H.; Astorga, C. Impact of Ethanol Containing Gasoline Blends on Emissions from a Flex-Fuel Vehicle Tested over the Worldwide Harmonized Light Duty Test Cycle (WLTC). *Fuel* **2015**, *143*, 173–182. [CrossRef]

67. Suarez-Bertoa, R.; Lähde, T.; Pavlovic, J.; Valverde, V.; Clairotte, M.; Giechaskiel, B. Laboratory and On-Road Evaluation of a GPF-Equipped Gasoline Vehicle. *Catalysts* **2019**, *9*, 678. [CrossRef]

68. Mehsein, K.; Norsic, C.; Chaillou, C.; Nicolle, A. Minimizing Secondary Pollutant Formation through Identification of Most Influential Volatile Emissions in Gasoline Exhausts: Impact of the Vehicle Powertrain Technology. *Atmos. Environ.* **2020**, *226*, 117394. [CrossRef]

69. Durbin, T.D.; Wilson, R.D.; Norbeck, J.M.; Miller, J.W.; Huai, T.; Rhee, S.H. Estimates of the Emission Rates of Ammonia from Light-Duty Vehicles Using Standard Chassis Dynamometer Test Cycles. *Atmos. Environ.* **2002**, *36*, 1475–1482. [CrossRef]

70. Woodburn, J.; Bielaczyc, P.; Szczotka, A. *Chassis Dynamometer Testing of Ammonia Emissions from Light-Duty Si Vehicles in the Context of Emissions of Reactive Nitrogen Compounds*; SAE Technical Paper 2013-01-1346: Warrendale, PA, USA, 2013. [CrossRef]

71. Suarez-Bertoa, R.; Zardini, A.A.; Astorga, C. Ammonia Exhaust Emissions from Spark Ignition Vehicles over the New European Driving Cycle. *Atmos. Environ.* **2014**, *97*, 43–53. [CrossRef]

72. Wang, X.; Ge, Y.; Gong, H.; Yang, Z.; Tan, J.; Hao, L.; Su, S. Ammonia Emissions from China-6 Compliant Gasoline Vehicles Tested over the WLTC. *Atmos. Environ.* **2019**, *199*, 136–142. [CrossRef]

73. Liu, Y.; Wang, H.; Li, N.; Tan, J.; Chen, D. Research on Ammonia Emissions from Three-Way Catalytic Converters Based on Small Sample Test and Vehicle Test. *Sci. Total Environ.* **2021**, *795*, 148926. [CrossRef]

74. Bogarra, M.; Herreros, J.M.; Tsolakis, A.; York, A.P.E.; Millington, P.J. Study of Particulate Matter and Gaseous Emissions in Gasoline Direct Injection Engine Using On-Board Exhaust Gas Fuel Reforming. *Appl. Energy* **2016**, *180*, 245–255. [CrossRef]

75. Clairotte, M.; Adam, T.W.; Zardini, A.A.; Manfredi, U.; Martini, G.; Krasenbrink, A.; Vicet, A.; Tournié, E.; Astorga, C. Effects of Low Temperature on the Cold Start Gaseous Emissions from Light Duty Vehicles Fuelled by Ethanol-Blended Gasoline. *Appl. Energy* **2013**, *102*, 44–54. [CrossRef]

76. Suarez-Bertoa, R.; Astorga, C. Isocyanic Acid and Ammonia in Vehicle Emissions. *Transp. Res. Part D Transp. Environ.* **2016**, *49*, 259–270. [CrossRef]

77. Huai, T.; Durbin, T.; Rhee, S.H.; Norbeck, J.M. Investigation of Emission Rates of Ammonia, Nitrous Oxide and Other Exhaust Compounds from Alternative Fuel Vehicles Using a Chassis Dynamometer. *Int. J. Automot. Technol.* **2003**, *4*, 9–19.

78. Reyes, F.; Grutter, M.; Jazcilevich, A.; González-Oropeza, R. Tecnical Note: Analysis of Non-Regulated Vehicular Emissions by Extractive FTIR Spectrometry: Tests on a Hybrid Car in Mexico City. *Atmos. Chem. Phys.* **2006**, *6*, 5339–5346. [CrossRef]

79. Suarez-Bertoa, R.; Astorga, C. Unregulated Emissions from Light-Duty Hybrid Electric Vehicles. *Atmos. Environ.* **2016**, *136*, 134–143. [CrossRef]

80. Suarez-Bertoa, R.; Pavlovic, J.; Trentadue, G.; Otura-Garcia, M.; Tansini, A.; Ciuffo, B.; Astorga, C. Effect of Low Ambient Temperature on Emissions and Electric Range of Plug-in Hybrid Electric Vehicles. *ACS Omega* **2019**, *4*, 3159–3168. [CrossRef]

81. Daemme, L.C.; Penteado, R.d.A.; Furlan, C.; Errera, M.; Zotin, F.M.Z. *An Investigation on Aldehyde and Ammonia Emissions from a 4-Stroke Gasoline-Fueled Motorcycle. Ammonia Emission Reduction by Using a SCR Catalyst*; SAE Technical Paper 2013-36-0181: Warrendale, PA, USA, 2013. [CrossRef]

82. Daemme, L.C.; Penteado, R.; Zotin, F.; Errera, M. *Regulated and Unregulated Emissions from a Flex Fuel Motorcycle Fuelled with Various Gasoline/Ethanol Blends*; SAE Technical Paper 2014-32-0032: Warrendale, PA, USA, 2014. [CrossRef]

83. Daemme, L.C.; Penteado, R.; Zotin, F.; Corrêa, S.M.; Errera, M.R.; Forcetto, A. *The Effect of Fuel Sulfur Content on Ammonia, Aldehyde and Regulated Emissions Emitted from a Euro Iii Motorcycle*; SAE Technical Paper 2016-36-0158: Warrendale, PA, USA, 2016. [CrossRef]

84. Clairotte, M.; Adam, T.W.; Chirico, R.; Giechaskiel, B.; Manfredi, U.; Elsasser, M.; Sklorz, M.; DeCarlo, P.F.; Heringa, M.F.; Zimmermann, R.; et al. Online Characterization of Regulated and Unregulated Gaseous and Particulate Exhaust Emissions from Two-Stroke Mopeds: A Chemometric Approach. *Anal. Chim. Acta* **2012**, *717*, 28–38. [CrossRef]

85. Zardini, A.A.; Platt, S.M.; Clairotte, M.; El Haddad, I.; Temime-Roussel, B.; Marchand, N.; Ježek, I.; Drinovec, L.; Močnik, G.; Slowik, J.G.; et al. Effects of Alkylate Fuel on Exhaust Emissions and Secondary Aerosol Formation of a 2-Stroke and a 4-Stroke Scooter. *Atmos. Environ.* **2014**, *94*, 307–315. [CrossRef]

86. Jetter, J.; Maeshiro, S.; Hatcho, S.; Klebba, R. *Development of an On-Board Analyzer for Use on Advanced Low Emission Vehicles*; SAE Technical Paper 2000-01-1140: Warrendale, PA, USA, 2000. [CrossRef]

87. Li, H.; Andrews, G.E.; Khan, A.A.; Savvidis, D.; Daham, B.; Bell, M.; Tate, J.; Ropkins, K. *Analysis of Driving Parameters and Emissions for Real World Urban Driving Cycles Using an On-Board Measurement Method for a Euro 2 SI Car*; SAE Technical Paper 2007-01-2066: Warrendale, PA, USA, 2007. [CrossRef]

88. Li, H.; Andrews, G.E.; Savvidis, D.; Daham, B.; Ropkins, K.; Bell, M.; Tate, J. *Comparisons of the Exhaust Emissions for Different Generations of SI Cars under Real World Urban Driving Conditions*; SAE Technical Paper 2008-01-0754: Warrendale, PA, USA, 2008. [CrossRef]

89. Khalfan, A.; Andrews, G.; Li, H. *Real World Driving: Emissions in Highly Congested Traffic*; SAE Technical Paper 2017-01-2388: Warrendale, PA, USA, 2017. [CrossRef]

90. Li, H.; Khalfan, A.; Andrews, G. Determination of GHG Emissions, Fuel Consumption and Thermal Efficiency for Real World Urban Driving Using a SI Probe Car. *SAE Int. J. Engines* **2014**, *7*, 1370–1381. [CrossRef]

91. Khalfan, A.; Li, H.; Andrews, G. Speciation of Nitrogen Compounds in the Tailpipe Emissions from a SI Car under Real World Driving Conditions. *SAE Int. J. Engines* **2014**, *7*, 1961–1983. [CrossRef]

92. Collins, J.F.; Shepherd, P.; Durbin, T.D.; Lents, J.; Norbeck, J.; Barth, M. Measurements of In-Use Emissions from Modern Vehicles Using an on-Board Measurement System. *Environ. Sci. Technol.* **2007**, *41*, 6554–6561. [CrossRef]

93. Li, H.; Andrews, G.E.; Savvidis, D.; Daham, B.; Ropkins, K.; Bell, M.; Tate, J.E. *Characterization of Regulated and Unregulated Cold Start Emissions for Different Real World Urban Driving Cycles Using a SI Passenger Car*; SAE Technical Paper 2008-01-1648: Warrendale, PA, USA, 2008. [CrossRef]

94. Li, H.; Andrews, G.E.; Savvidis, D.; Ropkins, K.; Tate, J.; Bell, M. *Investigation of Regulated and Non-Regulated Cold Start Emissions Using a Euro 3 SI Car as a Probe Vehicle under Real World Urban Driving Conditions*; SAE Technical Paper 2008-01-2428: Warrendale, PA, USA, 2008. [CrossRef]

95. Sentoff, K.M.; Robinson, M.K.; Holmén, B.A. Second-by-Second Characterization of Cold-Start Gas-Phase and Air Toxic Emissions from a Light-Duty Vehicle. *Transp. Res. Rec.* **2010**, *2158*, 95–104. [CrossRef]

96. Khalfan, A.; Li, H.; Andrews, G. *Cold Start SI Passenger Car Emissions from Real World Urban Congested Traffic*; SAE Technical Paper 2015-01-1064: Warrendale, PA, USA, 2015. [CrossRef]

97. Li, H.; Andrews, G.E.; Savvidis, D. Influence of Cold Start and Ambient Temperatures on Greenhouse Gas (GHG) Emissions, Global Warming Potential (GWP) and Fuel Economy for SI Car Real World Driving. *SAE Int. J. Fuels Lubr.* **2010**, *3*, 133–148. [CrossRef]

98. Vojtíšek-Lom, M.; Beránek, V.; Klír, V.; Jindra, P.; Pechout, M.; Voříšek, T. On-Road and Laboratory Emissions of NO, NO_2, NH_3, N_2O and CH_4 from Late-Model EU Light Utility Vehicles: Comparison of Diesel and CNG. *Sci. Total Environ.* **2018**, *616–617*, 774–784. [CrossRef]

99. Hadavi, S.A.; Li, H.; Przybyla, G.; Jarrett, R.; Andrews, G. Comparison of Gaseous Emissions for B100 and Diesel Fuels for Real World Urban and Extra Urban Driving. *SAE Int. J. Fuels Lubr.* **2012**, *5*, 1132–1154. [CrossRef]

100. Hadavi, S.; Andrews, G.E.; Li, H.; Przybyla, G.; Vazirian, M. *Diesel Cold Start into Congested Real World Traffic: Comparison of Diesel and B100 for Ozone Forming Potential*; SAE Technical Paper 2013-01-1145: Warrendale, PA, USA, 2013. [CrossRef]

101. Przybyla, G.; Hadavi, S.; Li, H.; Andrews, G.E. *Real World Diesel Engine Greenhouse Gas Emissions for Diesel Fuel and B100*; SAE Technical Paper 2013-01-1514: Warrendale, PA, USA, 2013. [CrossRef]

102. Suarez-Bertoa, R.; Pechout, M.; Vojtíšek, M.; Astorga, C. Regulated and Non-Regulated Emissions from Euro 6 Diesel, Gasoline and CNG Vehicles under Real-World Driving Conditions. *Atmosphere* **2020**, *11*, 204. [CrossRef]

103. Samaras, Z.; Andersson, J.; Aakko-Saksa, P.; Cuelenaere, R.; Mellios, G. Additional Technical Issues for Euro 7 (LDV). In Proceedings of the AGVES Webinar, Brussels, Belgium, 27 April 2021.

104. Vojtíšek, M.; Pechout, M. Portable, on-Board FTIR Spectrometers: A Universal Tool for Real-World Monitoring of Greenhouse Gases, Reactive Nitrogen Compounds, and Other Gaseous Pollutants? In Proceedings of the 24th International Transport and Air Pollution Conference Webinar, Graz, Austria, 30 March–1 April 2021.

105. Ligterink, N.; Vojtíšek, M.; Stelwagen, U.; von Goethem, S. On-Road Emission Measurements beyond Type Approval PEMS. In Proceedings of the 24th International Transport and Air Pollution Conference Webinar, Graz, Austria, 30 March–1 April 2021.

106. Giechaskiel, B.; Joshi, A.; Ntziachristos, L.; Dilara, P. European Regulatory Framework and Particulate Matter Emissions of Gasoline Light-Duty Vehicles: A Review. *Catalysts* **2019**, *9*, 586. [CrossRef]

107. Giechaskiel, B.; Clairotte, M.; Valverde-Morales, V.; Bonnel, P.; Kregar, Z.; Franco, V.; Dilara, P. Framework for the Assessment of PEMS (Portable Emissions Measurement Systems) Uncertainty. *Environ. Res.* **2018**, *166*, 251–260. [CrossRef] [PubMed]

108. Giechaskiel, B.; Bonnel, P.; Perujo, A.; Dilara, P. Solid Particle Number (SPN) Portable Emissions Measurement Systems (PEMS) in the European Legislation: A Review. *Int. J. Environ. Res. Public Health* **2019**, *16*, 4819. [CrossRef]

109. DieselNet Emission Standards 2021. Available online: https://dieselnet.com/standards (accessed on 11 August 2021).

110. Daham, B.; Andrews, G.E.; Li, H.; Ballesteros, R.; Bell, M.C.; Tate, J.; Ropkins, K. *Application of a Portable FTIR for Measuring On-Road Emissions*; SAE Technical Paper 2005-01-0676: Warrendale, PA, USA, 2005. [CrossRef]

111. White, J.U. Long Optical Paths of Large Aperture. *J. Opt. Soc. Am.* **1942**, *32*, 285. [CrossRef]

112. Kawarabayashi, S.; Yamagishi, Y.; Kachi, H.; Kobayashi, S. Measurement of Vehicle Emissions with Fourier Transform Infrared (FTIR) Method. *Int. Symp. COMODIA* **1990**, *90*, 365–369.

113. Baronick, J.; Heller, B.; Lach, G.; Luf, H. *Modal Measurement of Raw Exhaust Volume and Mass Emissions by SESAM*; SAE Technical Paper 980047: Warrendale, PA, USA, 1998. [CrossRef]

114. Adachi, M.; Inoue, K.; Yamagishi, Y.; Ishida, K. *Discussion of Operating Parameters and Analysis Capability for a Fourier Transform Infrared Emission Analyzer*; SAE Technical Paper 971018: Warrendale, PA, USA, 1997. [CrossRef]

115. Herget, W.F.; Staab, J.; Klingenberg, H.; Riedel, W.J. *Progress in the Prototype Development of a New Multicomponent Exhaust Gas Sampling and Analyzing System*; SAE Technical Paper 840470: Warrendale, PA, USA, 1984. [CrossRef]

116. Rothman, L.S.; Gordon, I.E. The HITRAN molecular database. In Proceedings of the AIP Conference Proceedings, Gaithersburg, MD, USA, 30 September–4 October 2012. [CrossRef]

117. Gordon, I.E.; Rothman, L.S.; Hill, C.; Kochanov, R.V.; Tan, Y.; Bernath, P.F.; Birk, M.; Boudon, V.; Campargue, A.; Chance, K.V.; et al. The HITRAN2016 Molecular Spectroscopic Database. *J. Quant. Spectrosc. Radiat. Transf.* **2017**, *203*, 3–69. [CrossRef]

118. Heland, J.; Schäfer, K. Determination of Major Combustion Products in Aircraft Exhausts by FTIR Emission Spectroscopy. *Atmos. Environ.* **1998**, *32*, 3067–3072. [CrossRef]

119. Zhao, Y.; Pan, Y.; Rutherford, J.; Mitloehner, F.M. Estimation of the Interference in Multi-Gas Measurements Using Infrared Photoacoustic Analyzers. *Atmosphere* **2012**, *3*, 246–265. [CrossRef]

120. Hoard, J.; Snow, R.; Xu, L.; Gierczak, C.; Hammerle, R.; Montreuil, C.; Farooq, S.I. *NOx Measurement Errors in Ammonia-Containing Exhaust*; SAE Technical Paper 2007-01-0330: Warrendale, PA, USA, 2007. [CrossRef]

121. Keens, A.; Simon, A. Correction of the Nonlinear Response of Infrared Detectors. In Proceedings of the 9th International Conference on Fourier Transform Spectroscopy, Calgary, AB, Canada, 23–27 August 1993; Proc. SPIE 2089. pp. 222–223. [CrossRef]

122. Russwurm, G.M.; Phillips, W. Uncertainties in FTIR Data Due to a Nonlinear Response. In Proceedings of the Photonics East (ISAM, VVDC, IEMB), Boston, MA, USA, 1–6 November 1998; Proc. SPIE 3534, Environmental Monioting and Remediation Technologies. pp. 176–186. [CrossRef]

123. Wallner, T.; Frazee, R. *Study of Regulated and Non-Regulated Emissions from Combustion of Gasoline, Alcohol Fuels and Their Blends in a DI-SI Engine*; SAE Technical Paper 2010-01-1571: Warrendale, PA, USA, 2010. [CrossRef]

124. Gautam, R.; Vanga, S.; Ariese, F.; Umapathy, S. Review of Multidimensional Data Processing Approaches for Raman and Infrared Spectroscopy. *EPJ Tech. Instrum.* **2015**, *2*, 1–38. [CrossRef]

125. Bacsik, Z.; Mink, J.; Keresztury, G. FTIR Spectroscopy of the Atmosphere. I. Principles and Methods. *Appl. Spectrosc. Rev.* **2004**, *39*, 295–363. [CrossRef]

126. Gierczak, C.A.; Andino, J.M.; Butler, J.W.; Heiser, G.A.; Jesion, G.; Korniski, T.J. FTIR: Fundamentals and Applications in the Analysis of Dilute Vehicle Exhaust. In Proceedings of the Optics, Elctro-Optics, and Laser Applications in Science and Engineering, Los Angeles, CA, USA, 20–25 January 1991; Proc. SPIE 1433, Measurement of Atmospheric Gases. pp. 315–328. [CrossRef]

127. Maricq, M. Exhaust emissions. In *Encyclopedia of Automotive Engineering*; Crolla, D., Foster, D.E., Kobayashi, T., Vaughan, N., Eds.; John Wiley & Sons, Ltd.: Chichester, UK, 2014; pp. 1–14. ISBN 978-1-118-35417-9.

128. Adachi, M.; Nakamura, H. *Engine Emissions Measurement Handbook: HORIBA Automotive Test Systems*; SAE International: Warrendale, PA, USA, 2014; ISBN 978-0-7680-8012-4.

129. Majewski, W.A.; Khair, M.K. *Diesel Emissions and Their Control*; SAE International: Warrendale, PA, USA, 2006; ISBN 978-0-7680-0674-2.

130. Kasab, J.J.; Strzelec, A. *Automotive Emissions Regulations and Exhaust Aftertreatment Systems*; SAE International: Warrendale, PA, USA, 2020; ISBN 978-0-7680-9955-3.

131. Sun, Y.-W.; Liu, W.-Q.; Zeng, Y.; Wang, S.-M.; Huang, S.-H.; Xie, P.-H.; Yu, X.-M. Water Vapor Interference Correction in a Non Dispersive Infrared Multi-Gas Analyzer. *Chin. Phys. Lett.* **2011**, *28*, 073302. [CrossRef]

132. Inoue, K.; Ishihara, M.; Akashi, K.; Adachi, M.; Ishida, K. *Numerical Analysis of Mass Emission Measurement Systems for Low Emission Vehicles*; SAE Technical Paper 1999-01-0150: Warrendale, PA, USA, 1999. [CrossRef]

133. Nakamura, H.; Kihara, N.; Adachi, M.; Ishida, K. *Development of a Wet-Based NDIR and Its Application to on-Board Emission Measurement System*; SAE Technical Paper 2002-01-0612: Warrendale, PA, USA, 2002. [CrossRef]

134. Dinh, T.-V.; Choi, I.-Y.; Son, Y.-S.; Kim, J.-C. A Review on Non-Dispersive Infrared Gas Sensors: Improvement of Sensor Detection Limit and Interference Correction. *Sens. Actuators B Chem.* **2016**, *231*, 529–538. [CrossRef]

135. Giechaskiel, B.; Zardini, A.A.; Clairotte, M. Exhaust Gas Condensation during Engine Cold Start and Application of the Dry-Wet Correction Factor. *Appl. Sci.* **2019**, *9*, 2263. [CrossRef]

136. Gluck, S.; Glenn, C.; Logan, T.; Vu, B.; Walsh, M.; Williams, P. Evaluation of NOx Flue Gas Analyzers for Accuracy and Their Applicability for Low-Concentration Measurements. *J. Air Waste Manag. Assoc.* **2003**, *53*, 749–758. [CrossRef]

137. Akard, M.; Nakamura, H.; Aoki, S.; Kihara, N.; Adachi, M. *Performance Results and Design Considerations for a New In-Use Testing Instrument*; SAE Technical Paper 2005-01-3606: Warrendale, PA, USA, 2005. [CrossRef]

138. Shah, S.D.; Mauti, A.; Richert, J.F.O.; Loos, M.J.; Chase, R.E. *Measuring NOx in the Presence of Ammonia*; SAE Technical Paper 2007-01-0331: Warrendale, PA, USA, 2007. [CrossRef]

139. Baronick, J.D.; Heller, B.; Lach, G.; Bogner, F.; Gerspach, U.; Schimpl, H.; Gruber, D.; Fabinski, W.; Moede, M.; Zöchbauer, M. *Evaluation of an UV Analyzer for NOx Vehicle Emission Measurement*; SAE Technical Paper 2001-01-0213: Warrendale, PA, USA, 2001. [CrossRef]

140. Czerwinski, J.; Comte, P.; Güdel, M.; Mayer, A.; Lemaire, J.; Reutimann, F.; Berger, A.H. *Investigations of NO$_2$ in Legal Test Procedure for Diesel Passenger Cars*; SAE Technical Paper 2015-24-2510: Warrendale, PA, USA, 2015. [CrossRef]

141. Arlitt, B. *Korrelationen NOx: NO, NO$_2$ Und NOx Analyse Mit FTIR Und CLD*; AVL List GmbH: Graz, Austria, 2018.

142. Olsen, D.B.; Kohls, M.; Arney, G. Impact of Oxidation Catalysts on Exhaust NO$_2$/NOx Ratio from Lean-Burn Natural Gas Engines. *J. Air Waste Manag. Assoc.* **2010**, *60*, 867–874. [CrossRef] [PubMed]

143. Meinel, H.; Just, T. Measurement of NOx Exhaust Emissions by a New NDUV Analyzer. In Proceedings of the 14th Aerospace Sciences Meeting, American Institute of Aeronautics and Astronautics, Washington, DC, USA, 26 January 1976.

144. Cao, T.; Durbin, T.D.; Cocker, D.R.; Wanker, R.; Schimpl, T.; Pointner, V.; Oberguggenberger, K.; Johnson, K.C. A Comprehensive Evaluation of a Gaseous Portable Emissions Measurement System with a Mobile Reference Laboratory. *Emiss. Control Sci. Technol.* **2016**, *2*, 173–180. [CrossRef]

145. Varella, R.; Giechaskiel, B.; Sousa, L.; Duarte, G. Comparison of Portable Emissions Measurement Systems (PEMS) with Laboratory Grade Equipment. *Appl. Sci.* **2018**, *8*, 1633. [CrossRef]

146. Ballantyne, V.F.; Howes, P.; Stephanson, L. *Nitrous Oxide Emissions from Light Duty Vehicles*; SAE Technical Paper 940304: Warrendale, PA, USA, 1994. [CrossRef]

147. Rahman, M.; Hara, K.; Nakatani, S.; Tanaka, Y. *Development of a Fast Response Nitrogen Compounds Analyzer Using Quantum Cascade Laser for Wide-Range Measurement*; SAE Technical Paper 2011-26-0044: Warrendale, PA, USA, 2011. [CrossRef]

148. Hara, K.; Nakatani, S.; Rahman, M.; Nakamura, H.; Tanaka, Y.; Ukon, J. *Development of Nitrogen Components Analyzer Utilizing Quantum Cascade Laser*; SAE Technical Paper 2009-01-2743: Warrendale, PA, USA, 2009. [CrossRef]

149. Murtonen, T.; Vesala, H.; Koponen, P.; Pettinen, R.; Kajolinna, T.; Antson, O. *NH$_3$ Sensor Measurements in Different Engine Applications*; SAE Technical Paper 2018-01-1814: Warrendale, PA, USA, 2018. [CrossRef]

150. Seykens, X.; van den Tillaart, E.; Lilova, V.; Nakatani, S. *NH$_3$ Measurements for Advanced SCR Applications*; SAE Technical Paper 2016-01-0975: Warrendale, PA, USA, 2016. [CrossRef]

151. Suarez-Bertoa, R.; Zardini, A.A.; Lilova, V.; Meyer, D.; Nakatani, S.; Hibel, F.; Ewers, J.; Clairotte, M.; Hill, L.; Astorga, C. Intercomparison of Real-Time Tailpipe Ammonia Measurements from Vehicles Tested over the New World-Harmonized Light-Duty Vehicle Test Cycle (WLTC). *Environ. Sci. Pollut. Res.* **2015**, *22*, 7450–7460. [CrossRef] [PubMed]

152. Mohn, J.; Forss, A.M.; Bruhlmann, S.; Zeyer, K.; Luscher, R.; Emmenegger, L.; Novak, P.; Heeb, N. Time-Resolved Ammonia Measurement in Vehicle Exhaust. *Int. J. Environ. Pollut.* **2004**, *22*, 342–356. [CrossRef]

153. Pisano, J.T.; Sauer, C.; Durbin, T.; Mackay, G. *Measurement of Low Concentration NH3 in Diesel Exhaust Using Tunable Diode Laser Adsorption Spectroscopy (TDLAS)*; SAE Technical Paper 2009-01-1519: Warrendale, PA, USA, 2009. [CrossRef]

154. McWilliam, I.G.; Dewar, R.A. Flame Ionization Detector for Gas Chromatography. *Nature* **1958**, *181*, 760. [CrossRef]

155. Cheng, W.K.; Summers, T.; Collings, N. The Fast-Response Flame Ionization Detector. *Prog. Energy Combust. Sci.* **1998**, *24*, 89–124. [CrossRef]

156. Palo, D.R.; Dagle, R.A.; Holladay, J.D. Methanol Steam Reforming for Hydrogen Production. *Chem. Rev.* **2007**, *107*, 3992–4021. [CrossRef]

157. Dietz, W.A. Response Factors for Gas Chromatographic Analyses. *J. Chromatogr. Sci.* **1967**, *5*, 68–71. [CrossRef]

158. Jorgensen, A.D.; Picel, K.C.; Stamoudis, V.C. Prediction of Gas Chromatography Flame Ionization Detector Response Factors from Molecular Structures. *Anal. Chem.* **1990**, *62*, 683–689. [CrossRef]

159. Wallner, T. Correlation between Speciated Hydrocarbon Emissions and Flame Ionization Detector Response for Gasoline/Alcohol Blends. *J. Eng. Gas Turbines Power* **2011**, *133*, 082801. [CrossRef]

160. Sandstroem-Dahl, C.; Erlandsson, L.; Gasste, J.; Lindgren, M. Measurement Methodologies for Hydrocarbons, Ethanol and Aldehyde Emissions from Ethanol Fuelled Vehicles. *SAE Int. J. Fuels Lubr.* **2010**, *3*, 453–466. [CrossRef]

161. Loo, J.F.; Parker, D.T. *Evaluation of a Photoacoustic Gas Analyzer for Ethanol Vehicle Emissions Measurement*; SAE Technical Paper 2000-01-0794: Warrendale, PA, USA, 2000. [CrossRef]

162. Gierczak, C.A.; Kralik, L.L.; Mauti, A.; Harwell, A.L.; Maricq, M.M. Measuring NMHC and NMOG Emissions from Motor Vehicles via FTIR Spectroscopy. *Atmos. Environ.* **2017**, *150*, 425–433. [CrossRef]

163. Li, H.; Ropkins, K.; Andrews, G.E.; Daham, B.; Bell, M.; Tate, J.; Hawley, G. *Evaluation of a FTIR Emission Measurement System for Legislated Emissions Using a SI Car*; SAE Technical Paper 2006-01-3368: Warrendale, PA, USA, 2006. [CrossRef]

164. Butler, J.W.; Maker, P.D.; Korniski, T.J.; Haack, L.P.; McKelvy, F.E.; Colvin, A.D. *A System for On-Line Measurement of Multicomponent Emissions and Engine Operating Parameters*; SAE Technical Paper 851657: Warrendale, PA, USA, 1985. [CrossRef]

165. Heller, B.; Klingenberg, H.; Lach, G.; Winckler, J. *Performance of a New System for Emission Sampling and Measurement (SESAM)*; SAE Technical Paper 900275: Warrendale, PA, USA, 1990. [CrossRef]

166. Shore, P.R.; deVries, R.S. *On-Line Hydrocarbon Speciation Using FTIR and CI-MS*; SAE Technical Paper 922246: Warrendale, PA, USA, 1992. [CrossRef]

167. Wright, N.; Osborne, D.; Music, N. *Comparison of Hydrocarbon Measurement with FTIR and FID in a Dual Fuel Locomotive Engine*; SAE Technical Paper 2016-01-0978: Warrendale, PA, USA, 2016. [CrossRef]

168. Suarez-Bertoa, R.; Clairotte, M.; Arlitt, B.; Nakatani, S.; Hill, L.; Winkler, K.; Kaarsberg, C.; Knauf, T.; Zijlmans, R.; Boertien, H.; et al. Intercomparison of Ethanol, Formaldehyde and Acetaldehyde Measurements from a Flex-Fuel Vehicle Exhaust during the WLTC. *Fuel* **2017**, *203*, 330–340. [CrossRef]

169. Rieger, P.L.; Maddox, C.E. Analysis of Exhaust from Clean-Fuel Vehicles Using FTIR Spectroscopy. In Proceedings of the Optics, Electro-Optics, and Laser Applications in Science and Engineering, Los Angeles, CA, USA, 20–25 January 1991; Proc. SPIE 1433, Measurement of Atmopheric Gases. pp. 290–301. [CrossRef]

170. McArver, A.Q. *Comparison of Data from Two FTIR Based Automotive Emissions Analysis Systems with Those Obtained from Conventional Automotive Emissions Instrumentation*; SAE Technical Paper 932660: Warrendale, PA, USA, 1993. [CrossRef]

171. Roberts, J.P.; Lowry, S.R. *Modal Measurements of Some Important NMOG Species by FT-IR Spectroscopy*; SAE Technical Paper 940739: Warrendale, PA, USA, 1994. [CrossRef]

172. Silva, K.C.C.; Daemme, L.C.; Macedo, V.d.C.; Penteado, R.d.A.; Ostapuik, I.F.; Corrêa, S.M. *Measurement of Legislated Emissions, Unburned Alcohol and Potential Formation of Ozone from a Light Flex-Fuel Vehicle*; SAE Technical Paper 2014-36-0260: Warrendale, PA, USA, 2014. [CrossRef]

173. Oberdorfer, P.E. *The Determination of Aldehydes in Automobile Exhaust Gas*; SAE Technical Paper 670123: Warrendale, PA, USA, 1967. [CrossRef]

174. Wagner, T.; Wyszyński, M.L. Aldehydes and Ketones in Engine Exhaust Emissions—A Review. *Proc. Inst. Mech. Eng. Part D J. Automob. Eng.* **1996**, *210*, 109–122. [CrossRef]

175. Williams, J.; Li, H.; Ross, A.B.; Hargreaves, S.P. Quantification of the Influence of NO_2, NO and CO Gases on the Determination of Formaldehyde and Acetaldehyde Using the DNPH Method as Applied to Polluted Environments. *Atmos. Environ.* **2019**, *218*, 117019. [CrossRef]

176. Shiotani, H.; Goto, S.; Kinoshita, K.; Nikolic, D. *Characteristics of Aldehydes and VOCs Emission from Off-Road Engines*; SAE Technical Paper 2006-32-0023: Warrendale, PA, USA, 2006. [CrossRef]

177. Shareef, G.S.; Ogle, L.; Ferry, K.; LaCosse, J.; Johnson, K.; McCarthy, J. Measurement of Aldehydes in Internal Combustion Engine Exhaust. In Proceedings of the SPE/EPA Exploration and Production Environmental Conference, Dallas, TX, USA, 3 March 1997; p. SPE-37878-MS.

178. Truex, T.J.; Collins, J.F.; Jetter, J.J.; Knight, B.; Hayashi, T.; Kishi, N.; Suzuki, N. *Measurement of Ambient Roadway and Vehicle Exhaust Emissions—An Assessment of Instrument Capability and Initial on-Road Test Results with an Advanced Low Emission Vehicle*; SAE Technical Paper 2000-01-1142: Warrendale, PA, USA, 2000. [CrossRef]

179. Zhang, F.; Wang, J.; Tian, D.; Wang, J.-X.; Shuai, S.-J. Research on Unregulated Emissions from an Alcohols-Gasoline Blend Vehicle Using FTIR, HPLC and GC-MS Measuring Methods. *SAE Int. J. Engines* **2013**, *6*, 1126–1137. [CrossRef]

180. Aakko, P.; Lappi, M.; Laurikko, J.; Nylund, N.-O. Experiences in Analyzing the Exhaust Gas Emissions of Vehicles Using Fast, on-Line FTIR. In Proceedings of the Nordic Seminar on Gas Analysis in Combustion, Tampere, Finland, 4–5 October 1994.

181. Liang, Y.; Tang, X.; Zhang, X.; Tian, F.; Sun, Y.; Dong, H. Portable Gas Analyzer Based on Fourier Transform Infrared Spectrometer for Patrolling and Examining Gas Exhaust. *J. Spectrosc.* **2015**, *2015*, 136516. [CrossRef]

182. Dasrath, D.; Frazee, R.; Hwang, J.; Northrop, W. *Comparison and Optimization of Fourier Transform Infrared Spectroscopy and Gas Chromatography-Mass Spectroscopy for Speciating Unburned Hydrocarbons from Diesel Low Temperature Combustion*; SAE Technical Paper 2017-01-0992: Warrendale, PA, USA, 2017. [CrossRef]

183. Lamas, J.E.; Hara, K.; Mori, Y. *Optimization of Automotive Exhaust Sampling Parameters for Evaluation of after-Treatment Systems Using FTIR Exhaust Gas Analyzers*; SAE Technical Paper 2019-01-0746: Warrendale, PA, USA, 2019. [CrossRef]

184. Woodburn, J. Emissions of Reactive Nitrogen Compounds (RNCs) from Two Vehicles with Turbo-Charged Spark Ignition Engines over Cold Start Driving Cycles. *Combust. Engines* **2021**. [CrossRef]

185. Hoard, J.; Venkataramanan, N.; Marshik, B.; Murphy, W. *NH_3 Storage in Sample Lines*; SAE Technical Paper 2014-01-1586: Warrendale, PA, USA, 2014. [CrossRef]

186. Herget, W.F.; Brasher, J.D. Remote Fourier Transform Infrared Air Pollution Studies. *Opt. Eng* **1980**, *19*. [CrossRef]

187. Balaji, P.S.; Rahman, M.E.; Moussa, L.; Lau, H.H. Wire Rope Isolators for Vibration Isolation of Equipment and Structures—A Review. *IOP Conf. Ser. Mater. Sci. Eng.* **2015**, *78*, 012001. [CrossRef]

188. Köhler, M.; Schardt, M.; Rauscher, M.; Koch, A. Gas Measurement Using Static Fourier Transform Infrared Spectrometers. *Sensors* **2017**, *17*, 2612. [CrossRef]

189. Valverde, V.; Giechaskiel, B.; Carriero, M. *Real Driving Emissions: 2018–2019 Assessment of Portable Emissions Measurement Systems (PEMS) Measurement Uncertainty*; Publications Office: Luxembourg, 2020.

190. CEN/TS 17507:2021. *Road Vehicles—Portable Emission Measuring Systems (PEMS)—Performance Assessment*; BSI: London, UK, 2021.

191. CEN/TS 17337:2019. *Stationary Source Emissions. Determination of Mass Concentration of Multiple Gaseous Species. Fourier Transform Infrared Spectroscopy*; BSI: London, UK, 2019; ISBN 978-0-580-51513-2.

192. SAE J2992. *FTIR Gas Analyzer Performance Evaluation/Qualification for Automotive Testing*; SAE International: Warrendale, PA, USA, 2020.

193. ASTM D6348 D22 Committee. *Test Method for Determination of Gaseous Compounds by Extractive Direct Interface Fourier Transform Infrared (FTIR) Spectroscopy*; ASTM International: West Conshohocken, PA, USA, 2020.

194. EPA. *Method 320: Measurement of Vapor Phase Organic and Inorganic Emissions by Extractive Fourier Transform Infrared (FTIR) Spectroscopy*; EPA: Washington, DC, USA, 2020.

195. Miers, S.A.; Green, C.; Meldrum, J.; Chmielewski, M. Measurement of Regulated and Unregulated Exhaust Emissions from Snowmobiles in the 2009 SAE Clean Snowmobile Challenge. *SAE Int. J. Fuels Lubr.* **2010**, *3*, 1112–1121. [CrossRef]

196. Kumar, A.; Arlitt, B.; Jacksier, T. *Effects of Isotopic Calibration Gases on IR Quantification Analyzer Techniques to Measure CO and CO_2 in Engine Emissions Testing*; SAE Technical Paper 2019-01-0076: Warrendale, PA, USA, 2019. [CrossRef]

197. Aakko-Saksa, P.; Roslund, P.; Koponen, P. *Development and Validation of Comprehensive Emission Measurement Methods for Alternative Fuels at VTT*; VTT: Helsinki, Finland, 2017; p. 102.

198. Valverde, V.; Giechaskiel, B. Assessment of Gaseous and Particulate Emissions of a Euro 6d-Temp Diesel Vehicle Driven >1300 Km Including Six Diesel Particulate Filter Regenerations. *Atmosphere* **2020**, *11*, 645. [CrossRef]

199. Giechaskiel, B.; Valverde, V.; Kontses, A.; Suarez-Bertoa, R.; Selleri, T.; Melas, A.; Otura, M.; Ferrarese, C.; Martini, G.; Balazs, A.; et al. Effect of Extreme Temperatures and Driving Conditions on Gaseous Pollutants of a Euro 6d-Temp Gasoline Vehicle. *Atmosphere* **2021**, *12*, 1011. [CrossRef]

200. Li, N.; El-Hamalawi, A.; Barrett, R.; Wheatley, A.; Robinson, J. Nitrogen Species Measurement Investigation Using Two Different FTIR. In Proceedings of the 18th IASTEM International Conference; International Academy of Science, Technology, Engnineering and Management, Berlin, Germany, 29 March 2016; pp. 24–29.

201. Suarez-Bertoa, R.; Mendoza-Villafuerte, P.; Riccobono, F.; Vojtisek, M.; Pechout, M.; Perujo, A.; Astorga, C. On-Road Measurement of NH_3 Emissions from Gasoline and Diesel Passenger Cars during Real World Driving Conditions. *Atmos. Environ.* **2017**, *166*, 488–497. [CrossRef]

202. Livingston, C.; Rieger, P.; Winer, A. Ammonia Emissions from a Representative In-Use Fleet of Light and Medium-Duty Vehicles in the California South Coast Air Basin. *Atmos. Environ.* **2009**, *43*, 3326–3333. [CrossRef]

203. Penteado, R.; Daemme, L.; Melo, T. *An Experimental Investigation on Regulated and Unregulated Emissions from Four 4-Stroke Gasoline-Powered Motorcycle*; SAE Technical Paper 2012-01-1098: Warrendale, PA, USA, 2012. [CrossRef]

204. Li, N.; El-Hamalawi, A.; Barrett, R.; Baxter, J. *Ammonia Measurement Investigation Using Quantum Cascade Laser and Two Different Fourier Transform Infrared Spectroscopy Methods*; SAE Technical Paper 2020-01-0365: Warrendale, PA, USA, 2020. [CrossRef]

205. Daemme, L.C.; Penteado, R.; Corrêa, S.M.; Zotin, F.; Errera, M.R. Emissions of Criteria and Non-Criteria Pollutants by a Flex-Fuel Motorcycle. *J. Braz. Chem. Soc.* **2016**, *27*, 2192–2202. [CrossRef]